Norwegian University
of Life Sciences

Master's Thesis 2023 30 ECTS
Faculty of Science and Technology

Recent advances in direct ammonia fuel cells and systems: a literature review

Mari Saure Bogen
Environmental Physics and Renewable Energy

Abstract

Ammonia has over the last two decades emerged as a promising carbon-free energy carrier due to its higher volumetric energy density and more widely developed distribution infrastructure compared to hydrogen. This makes ammonia a more encouraging alternative with regard to transportation and energy storage in a low-carbon energy future.

The direct use of ammonia in fuel cells has been investigated through a literature review on solid oxide fuel cells (proton conducting (PCFC) and oxide ion conducting (SOFC-O)), and anion exchange membrane (AEMFC) fuel cell technologies. The study has been executed with a particular focus on the most recent advances, in addition to a mapping of which challenges to overcome to enable commercial relevance for these technologies.

Oxide ion conducting SOFC-O stands out as the most mature technology for ammonia, with performances similar to H_2 in larger systems. The proton-conducting PCFC is following close behind with equivalent peak power densities as SOFC-O at cell-level. However, the scale-up within PCFC has not yet been reported for ammonia-fed PCFC. Stability and durability are challenges for both solid oxide technologies, where nickel nitriding is the major degradation mechanism. Another hindrance is the unsatisfactory ammonia decomposition at lowered operating temperatures.

The anion exchange membrane fuel cell emerges as a promising, yet immature low-temperature technology that has shown considerable advancements in the last decade. The most notable challenges here are slow ammonia oxidation, membrane stability problems, a significant amount of fuel crossover, and poor interface charge transfer between the electrodes and the membrane.

Samandrag

Ammoniakk har dei to siste tiåra opplevd aukande interesse som energiberar grunna den høgare volumetriske energitettheita og meir velutvikla infrastrukturen for distribusjon, samanlikna med hydrogen. Dette gjer ammoniakk til eit lovande alternativ for transport og energilagring i ei lågkarbon energiframtid.

Bruk av ammoniakk direkte i brenselceller har blitt undersøkt ved å utføre eit litteraturstudie på brenselcelleteknologiane fastoksid-brensellceller (protonledande (PCFC) og oksid-ionledande (SOFC-O)) samt anionledande membran brenselcelle (AEMFC). Studiet har blitt utført med eit ekstra fokus på dei nyaste framskritta innan desse teknologiane, samt ei vurdering av kva utfordringar som er mest kritiske å overkomme for å oppnå kommersiell relevans.

SOFC-O står fram som den mest modne tenknologien, med vellykka prestasjonar på linje med hydrogendrift også i større system. Dei protonledande fastoksidcellene følger tett på, med tilsvarande prestasjonar på cellenivå. Til motsetning har ikkje større PCFC system med ammoniakk blitt rapportert om enno. Både stabilitet og durabilitet er eit problem for begge fastoksidteknologier, kor nitridering av nikkel står ut som den største årsaken til degradering. Eit anna hinder er utilfredsstillande dekomponering av ammoniakk ved lågare temperaturar.

AEMFC er ein forholdsvis umoden ny lågtemperatur teknologi, men har vist enorme framsteg berre det siste tiåret. Dei mest framtredande utfordringane her er langsom oksidasjon av ammoniakk, stabilitetsproblem i membranen som fører til aukande grad av ammoniakk som kryssar fra anode til katode, samt dårleg ladningsoverføring mellom elektroder og membran.

Acknowledgements

First, I want to thank Professor Jorge Marchetti for invaluable guidance, for always keeping the door open for questions, and for encouraging curiosity and critical thinking, two essential qualities when writing a literature review.

Professor Truls Norby, thank you for generously sharing your time and vast knowledge, and for truly interesting discussions.

Erik Hektor, thank you for your valuable feedback and the possibility of doing some of my work at DNV.

I would also like to send my gratitude to Arne Auen Grimenes, who welcomed us all here in our first year. I am sure you have awoken the interest in physics of hundreds of students throughout the years. Thank you for your sincere enthusiasm. The study programme would never have become what it is today without you.

This thesis marks my final days as a student at NMBU, which in addition to (what feels like) endless studying hours have included joyful lunch breaks, late evenings, and close friendships. I want to send a special thanks to my classmates and good friends for all the fun and for the journey it has been to grow and learn together through five years. I am so proud of us.

Lastly, a big thanks to my near and dear for always being my supporters, and to Hogne, who simply is the best.

Contents

List of Figures

List of Tables

Acronyms

ADR Ammonia Decomposition Reaction.

AEMFC Anion Exchange Membrane Fuel Cell.

AOR Ammonia Oxidation Reaction.

BSCF Barium Strontium Cobalt Ferrite.

BZCY Yttria-doped Barium Zirconate.

BZCYYb Yttrium-and Ytterbium-doped Barium-zirconium-cerate.

CHP Combined Heat and Power.

DA Direct Ammonia.

GDC Gadolinia-doped Ceria.

HOR Hydrogen Oxidation Reaction.

LSC Lanthanum Strontium Cobalt.

LSCF Lanthanum Strontium Cobalt Ferrite.

LSM Lanthanum Strontium Manganite.

MIEC Mixed Ionic Electronic Conductor.

NCAL $LiNi_{0.815}Co_{0.15}Al_{0.035}O_2$.

OCV Open Circuit Voltage.

ORR Oxygen Reduction Reaction.

PCFC Protonic Ceramic Fuel Cell.

PEMFC Proton Exchange Membrane Fuel Cell.

PPD Peak Power Density.

PTFE Polytetrafluoroethylene.

QA Quaternary Ammonium.

SDC Samarium-doped Ceria.

SOFC Solid Oxide Fuel Cell.

SOFC-O Oxide ion conducting Solid Oxide Fuel Cell.

SSZ Scandia-stabilised Zirconia.

TPB Triple-phase Boundary.

YSZ Yttria-stabilised Zirconia.

CHAPTER 1

Introduction

1.1 Background

With about 80% of the world's energy demand still being covered by fossil fuels in 2022 [1], the fast-forwarding of carbon-free energy technology is critical for humanity to reduce greenhouse gas emissions (GHG) and ultimately mitigate climate change. Continuous electrification efforts are currently taking place across the globe, together with an increase in the installation of variable renewable energy sources such as wind and solar [2]. This evolution has incentivised an increase in research and development of fuel cell technology, utilising hydrogen for energy storage- and conversion purposes as well as for transportation. Even though hydrogen and fuel cell technology are gaining momentum [1], this technology is not new. Fuel cells, devices that convert chemical energy from a fuel into electricity through redox reactions, have their origin in the mid-1800s when William Grove found that electricity could be generated through electrochemical reactions between hydrogen and oxygen over platinum electrodes [3]. The commercialisation of fuel cells came in the 1960s when NASA used hydrogen-fed Proton Exchange Membrane Fuel Cell (PEMFC) and alkaline fuel cells to provide electricity and fresh water for astronauts in spacecraft [4]. Since then, and particularly in recent years, fuel cells have been developed for a variety of applications including propulsion for planes, locomotives and road- and seagoing vehicles as well as for distributed power generation [5, 6].

Hydrogen is considered the preferred fuel for fuel cells and is regarded as a crucial component to reaching a net-zero emission energy future, as it is a carbon-free and scalable

energy carrier [5]. However, there are several challenges connected with hydrogen utilisation. The low volumetric energy density, low boiling point, and wide ignition range make hydrogen a demanding energy carrier to store and transport. Finding denser hydrogen carriers, preferably without carbon, has therefore been highly prioritised. Ammonia (NH_3) has stood out as one of the most promising alternatives, much due to the extensive infrastructure and competence already available to handle ammonia, as it is the second most produced chemical, globally [7]. Also, from a techno-economic analysis, ammonia is stated to be the least expensive fuel when compared to, amongst others, hydrogen, natural gas and petroleum [8].

Ammonia can easily be liquefied (room temperature/10 Bar) and holds almost 70% more energy per volume than liquid hydrogen [3]. Once liquefied, ammonia can solely be a hydrogen-storing medium or be used directly as a fuel. Solid Oxide Fuel Cells (SOFCs) and alkaline electrolyte fuel cells are currently the most promising fuel cells to run on ammonia as a direct fuel [9]. Extensive research has been done on ammonia fuel cells in recent years, testing various materials to obtain durable and effective operation for different applications. Utilising ammonia directly in fuel cell technology can greatly improve efficiency in fuel cell systems by excluding the need for ammonia crackers, and provide a clean and reliable substitute for fossil fuels.

1.2 Motivation and research questions

While hydrogen fuel cells are well commercialised, ammonia fuel cells have, despite extensive research, not yet managed to reach full technological readiness [7]. The commercialisation of ammonia fuel cell systems is at its dawn, but successful demonstrations of ammonia-fed fuel cell systems have recently been done [10]. The most promising fuel cell technologies capable of using ammonia directly without external decomposition are shown in Figure 1.1.

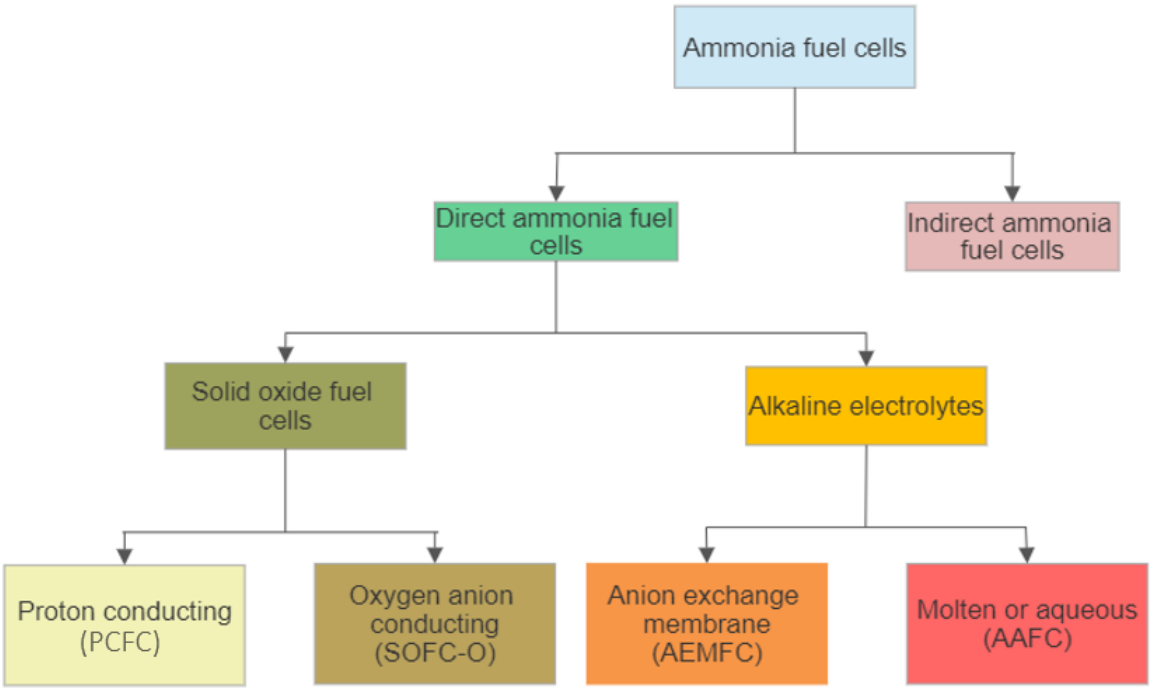

Figure 1.1: A schematic of the different classifications of ammonia fuel cells in accordance with Dincer and Siddiqui [3]. Modified with permission.

Several reviews on Direct Ammonia (DA) fuel cells have been published in recent years [9, 11–17]. From these reviews, covering the advances up until 2021, Oxide ion conducting Solid Oxide Fuel Cell (SOFC-O) is standing out as the most mature and efficient direct ammonia fuel cell technology, performing best with regard to power density. Protonic Ceramic Fuel Cell (PCFC) was stated to be the most promising next-generation ammonia fuel cell technology by Jeehr et al. [11], as they show great potential for lower temperature operation, which can prolong cell life. Moreover, proton-conducting support materials in the anode had higher decomposition activity of ammonia compared to that of SOFC-O [12]. However, until 2021, PCFC still yielded lower performances than SOFC-O. For Anion Exchange Membrane Fuel Cells (AEMFCs), record-high performances were achieved in 2018 [18], demonstrating promising, yet immature, low-temperature fuel cell technology.

A look into the latest progress within direct ammonia fuel cell technology is highly motivated by the fast progress in the field. A particular focus will be given to research from 2021 until recently (Feb 2023) to cover the most up-to-date advances within direct

ammonia fuel cells and evaluate their technological readiness. To encompass a variety of potential applications, low-temperature AEMFC and the two types of high-temperature solid oxide fuel cells are chosen for the review.

The core of the thesis encompasses two main research questions:

1. What is the recent progress in direct ammonia solid oxide- and alkaline membrane fuel cell technology?
2. What are the current challenges and future prospects for the given technologies?

1.2.1 Limitations

Fuel cells and their operation encompasses a wide variety of topics, which calls for some limitations for the scope of the thesis. As previously stated, the core of the thesis is directed towards ammonia-specific operation, and as the cathode working is similar regardless of the fuel fed to the cell, the main focus will instead be on the anode and the processes occurring here. Detailed manufacturing techniques and microstructure of materials, e.g grain sizes, pore structures and crystalline facets, fall outside the scope of the thesis and is only briefly discussed. Operational thermodynamic factors such as flow rates, mass transport, and fuel cell pressure are important aspects when optimising fuel cell performance. The effects of these factors will be touched upon, but a further elaboration on fuel cell performance based on these factors will not be given. Rather, the focus is directed towards the cells themselves and how their materials work with ammonia specifically.

1.2.2 Organisation of the review

For the literature search, articles on ammonia fuel cells have been assessed through Elsevier's database, Scopus. Newer articles (2021-) on direct ammonia fuel cells were emphasised the most, and also experimental studies were prioritised over modelling studies. Some articles describing the indirect use of ammonia in fuel cells were also included to look further into larger-scale systems to evaluate commercial-scale advancements.

The literature review comprises papers, reviews, books and press releases, with the goal of presenting state-of-the-art for direct ammonia solid oxide fuel cells and anion exchange

membrane fuel cells. First, a presentation of ammonia from an energy perspective is given, followed by descriptions of the three fuel cell technologies relevant. The criteria on which the fuel cell performance is evaluated will also be described. Further, recent research and progress, and systems and applications are presented before future prospects are discussed.

CHAPTER 2

Theory

2.1 Ammonia

2.1.1 Properties

Ammonia is a pungent-smelling, corrosive and toxic chemical compound, primarily known for its use in fertiliser production. Today, the amount of ammonia used for energy purposes accounts for a negligible part of the yearly produced 185 Mt (2020) [19]. However, ammonia has several attributes that make it suitable for speeding up the implementation of hydrogen in the energy mix, potentially providing a solution to several of the drawbacks of hydrogen [20]. Ammonia has a boiling point at -33°C at 1 atm, compared to hydrogen with -253°C at the same pressure, demanding less energy for liquefaction, hence providing more energy- and space-efficient hydrogen storage. Table 2.1 shows some physical properties of liquid ammonia compared to liquid and compressed hydrogen.

Table 2.1: Some physical properties of different hydrogen and ammonia states.

	Temperature [**°C**]	**Pressure [MPa]**	**H_2 density** [**kgH_2/m^3**]	**Energy density** [**GJ/m^3**]
H_2, compressed	25	35	26	2.76
H_2, compressed	25	70	42	5.60
H_2, liquid	-253	0.1	70	8.6
NH_3, liquid	25	1	121	12.7

Compared to gasoline, liquid ammonia has approximately 40% lower energy density with 18.6 GJ/t and 12.7 GJ/m^3 on mass and volume basis, respectively [19]. Furthermore, ammonia has a low flame speed and high ignition energy compared to gasoline [21]. Nevertheless, ammonia internal combustion engines and gas turbines are currently being developed [22], motivated by the fact that ammonia is carbon-free at the point of use.

2.1.2 Production

Production of ammonia most commonly entails the Haber-Bosch process, where nitrogen from air and hydrogen is combined over a Fe-based catalyst under high temperature (∼500°C) and pressure (>100 Bar) according to the reversible reaction 2.1 [23]

$$N_2 + 3H_2 \longleftrightarrow 2NH_3 \tag{2.1}$$

The hydrogen in this process is normally obtained from natural gas through steam methane reforming (SMR). SMR combines methane purified from natural gas with steam at high temperature (∼800°C) [7] to produce syngas (hydrogen and carbon monoxide (CO)) as shown in Equation 2.2

$$CH_4 + H_2O \longrightarrow CO + 3H_2 \tag{2.2}$$

From here, CO is eliminated and utilised for further hydrogen production through the water-gas shift reaction as in Equation 2.3

$$CO + H_2O \longrightarrow CO_2 + H_2 \tag{2.3}$$

The mentioned process accounts for about 70% of ammonia production [19], producing what is referred to as *grey* ammonia. Other fossil sources, such as coal, are also used as feedstock for hydrogen in ammonia production. In total, over 90% of ammonia is produced from hydrogen obtained from fossil sources, which generates large amounts of GHG emissions. 1.3% of 2020 global annual CO_2 emissions came from ammonia production, and also accounted for 2% of global energy use the same year [19].

The production of ammonia can broadly be divided into three colour categories - *grey*, as described, in addition to *blue* and *green*- based on how the hydrogen is obtained, as shown in Figure 2.1.

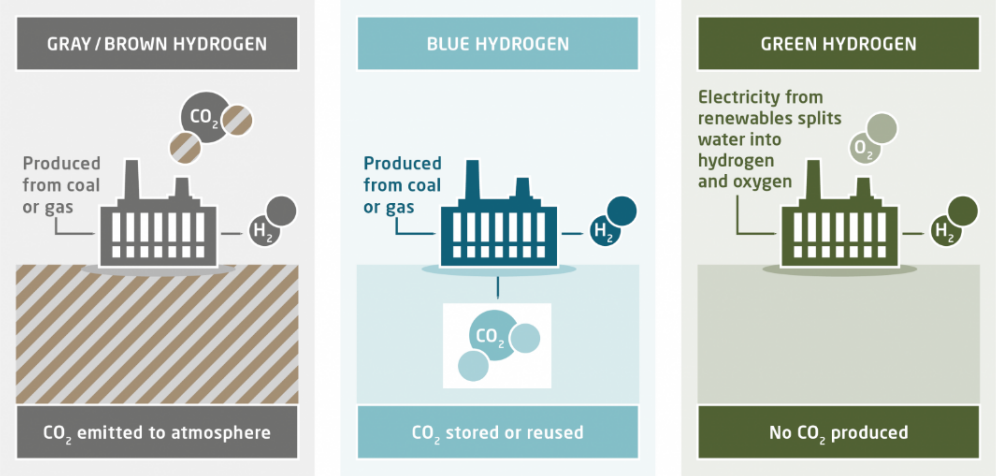

Figure 2.1: Different production pathways of hydrogen and the associated colours. Reprinted with permission [24].

Ammonia for energy purposes is mostly relevant if produced in a green manner, eliminating natural gas as hydrogen feedstock. Instead, hydrogen obtained through water-electrolysis powered by renewable energy, followed by the Haber-Bosch process can be done to produce green ammonia. This is a slightly more energy-demanding process compared to conventional production, yet it is relevant as there are no GHG emissions connected to the production [25].

Blue ammonia, comprising conventional hydrogen production with carbon capture and storage, is a method with fewer emissions than conventional and is seen as a useful production method in a transitional phase towards green hydrogen implementation [26, 27]. As the renewable share of the grid electricity mix is growing, so does the possibility of increased green hydrogen production.

2.2 Fuel cell basics

A fuel cell comprises three key elements; a negative electrode (anode), a positive electrode (cathode) and an ion-conducting medium between the two, the electrolyte. Figure 2.2 shows a simplified schematic of the most prominent fuel cell to date; the PEMFC.

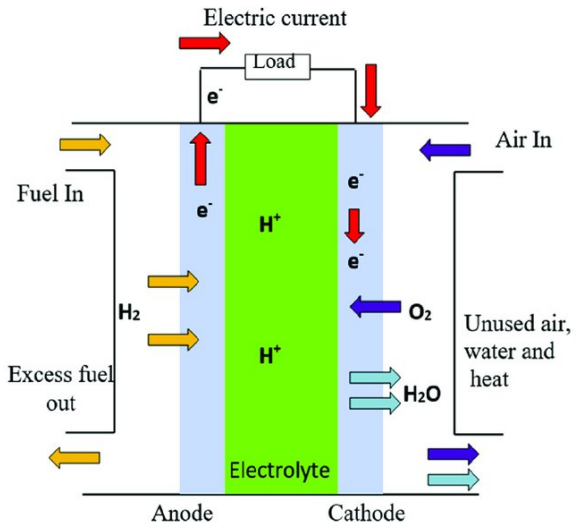

Figure 2.2: A simplified schematic of a PEM fuel cell. Reprinted from Li et al. [28], open access.

As seen in Figure 2.2, two types of charge transfer are seen in the system; electronic (e^-), through an external circuit and ionic (H^+) through the electrolyte. The migration of charges is driven by the potential differences between the anode and the cathode caused by redox reactions. Fuel (H_2 in this case) is fed to the anode, where it is oxidised into H^+ ions (protons) and releases electrons as shown in Equation 2.4.

$$2H_2 \longrightarrow 4H^+ + 4e^- \tag{2.4}$$

At the other side of the electrolyte, air is fed to the cathode, and O_2 is reduced to O^{2-} by reacting with the incoming electrons in the Oxygen Reduction Reaction (ORR). Further, water is formed with the protons that have migrated through the electrolyte as in Equation 2.5

$$O_2 + 4e^- + 4H^+ \longrightarrow 2H_2O \tag{2.5}$$

By combining the two half-reactions the complete overall fuel cell reaction becomes:

$$H_2 + \frac{1}{2}O_2 \longrightarrow H_2O \tag{2.6}$$

2.2.1 Fuel cell stacks

A single fuel cell does not generate enough voltage for most practical purposes, therefore several fuel cells are stacked together in an assembly to increase power output. The fuel cells are interconnected to enable electron flow through the stack. A planar geometry, relying on flat plate structured fuel cells often uses a bipolar stack design [29]. A bipolar plate ensures the electrical interconnection between the anode in one cell and the cathode in the next, while simultaneously feeding the cathode and anode oxygen and fuel, respectively [30]. Tubular geometries can commonly be seen in SOFC, where tubes are stacked with a interconnect material between the tubes [30].

2.2.2 Ammonia in fuel cells

When ammonia is used as a fuel instead of hydrogen, there are two ways to utilise the fuel; 1) Ammonia is utilised in a two-step process. First NH_3 is decomposed into H_2/N_2, as in Equation 2.7, before H_2 is oxidised as described in the previous section. The onset of thermal cracking of ammonia happens at around 400 °C, and for full dissociation (99.95%), temperatures at around 550-600 °C are sufficient in the presence of a catalyst [31]. 2) Ammonia is directly oxidised in the Ammonia Oxidation Reaction (AOR) as shown in Equation 2.8.

$$\mathrm{NH_3} \longrightarrow \frac{1}{2}\mathrm{N_2} + \frac{3}{2}\mathrm{H_2} \tag{2.7}$$

$$2\mathrm{NH_3} + \frac{3}{2}\mathrm{O_2} \longrightarrow 3\mathrm{H_2O} + \mathrm{N_2} \tag{2.8}$$

Both of these reactions show only the start and end products, but in reality, the processes entail several steps. The Ammonia Decomposition Reaction (ADR) steps are summed up in Table 2.2, while the AOR steps are shown in Table 2.3

Table 2.2: Ammonia decomposition steps [32].

Reaction	Explanation
$NH_3 + * \rightarrow NH_{3,ad}$	adsorption of NH_3
$NH_{3,ad} \rightarrow NH_{2,ad} + H_{ad}$	dehydrogenation step
$NH_{2,ad} \rightarrow NH_{ad} + H_{ad}$	dehydrogenation step
$2N_{ad} \rightarrow N_{2,ad}$	formation of N_2 molecules
$N_{2,ad} \rightarrow N_2 + *$	N_2 desorption
$2H_{ad} \rightarrow H_2 + *$	H_2 desorption

* denotes available adsorption cite at the catalyst surface

Table 2.3: Ammonia oxidation process steps in an alkaline fuel cell on platinum electrodes [14].

Reaction	Explanation
$NH_{3,ad} + OH^- \rightarrow NH_{2,ad} + H_2O + e^-$	dehydrogenation step
$NH_{2,ad} + OH^- \rightarrow NH_{ad} + H_2O + e^-$	dehydrogenation step
$2NH_{ad} \rightarrow N_2H_{2,ad}$	rate limiting step
$N_2H_{2,ad} + OH^- \rightarrow N_2H_{ad} + H_2O + e^-$	dehydrogenation step
$N_2H_{ad} + OH^- \rightarrow N_2 + H_2O + e^-$	final dehydrogenation step

The rate-limiting step is dependent on the catalyst applied. For the two common catalyst materials Ru and Ni, the rate-limiting step of ammonia decomposition has been shown to be the desorption of N_2, and the dehydrogenation process, respectively [33]. However, the decomposition is also dependent on several factors such as temperature, fuel flow rates and fuel mix composition and concentrations, as well as catalyst material structure [32].

2.2.3 Electrodes

In short, electrodes need to 1) facilitate their respective reactions, 2) ensure sufficient transport of electrons to the circuit and ions to the electrolyte, and 3) enable proper reactant and product diffusion to and from the active sites. Anode reactions include AOR or Hydrogen Oxidation Reaction (HOR), while ORR occurs at the cathode. More specifically, these reactions occur at the Triple-phase Boundary (TPB), the point where the reactants (H_2 or O_2) meet both the electrode and the electrolyte [34]. To maximise the active sites for electrode reactions and ensure sufficient reactant transport, electrodes

are made highly porous. This can be achieved by grinding, pressing and sintering nanostructured powders [34]. Further, catalytic materials are dispersed at the electrodes, to increase reaction rates.

In addition to high activity towards their respective reactions, the electrodes need to exhibit stability under a variety of operating conditions as well as chemical and mechanical compatibility with the electrolyte [35].

2.2.4 Electrolyte

The most important quality of an electrolyte is high ionic conductivity, but it should also possess some other important characteristics; it should not allow for gas diffusion between the anode and the cathode, it should have negligible electronic conductivity, and it must be chemically stable under a variety of operating conditions [35]. Mechanical compatibility with the electrodes is also crucial to prevent delamination at the electrode/electrolyte interface. This is often ensured by having some electrolyte material in the electrodes.

2.3 Fuel cell performance metrics

In order to quantify and compare the performances of the different fuel cells, some fundamental electrochemistry and fuel cell thermodynamics are presented.

2.3.1 Reversible cell voltage

The reversible voltage (E_r), also called Open Circuit Voltage (OCV) refers to the theoretical maximum voltage a fuel cell can provide under given operational conditions and can be found through Equation 2.9

$$\mathrm{E_r} = \frac{-\Delta \mathrm{G}}{\mathrm{zF}} \tag{2.9}$$

Here, ΔG is the change in Gibbs free energy, F is Faraday's constant, and z is the number of moles of electrons involved in the fuel cell reaction.

For fuel cells where NH_3 is decomposed, and H_2/O_2 takes part in the electrochemical reaction, the reversible voltage is 1.23 V under standard conditions (25°C, 1 atm) [3]. For

fuel cells where ammonia is directly oxidised, the calculated OCV is 1.17 V under the same standard conditions [36].

ΔG is a fundamental quantity, as it defines the amount of energy available to do work in a chemical reaction, hence is directly connected with fuel cell performance [29]. Considering the generic chemical reaction

$$\mathrm{qA} + \mathrm{rB} \longrightarrow \mathrm{sC} + \mathrm{tD}$$

where q, r, s and t represent stoichiometric coefficients of chemical compounds A, B, C and D, respectively, ΔG can be calculated through Equation 2.10

$$\Delta \mathrm{G} = \Delta \mathrm{G}^{\circ} + \mathrm{RTln}\left(\frac{\mathrm{a_C^q a_D^r}}{\mathrm{a_A^s a_B^t}}\right) \tag{2.10}$$

ΔG° denotes the change in Gibbs free energy under standard conditions, R is the ideal gas constant, and T is the temperature in Kelvin. The logarithmic term gives the relation between the product and reactant *activities (a)*. Activity is a unitless thermodynamic measure and is often referred to as "effective concentration" [29]. The activity of a species takes into account how much the actual partial pressure (in gas mixtures) or concentration (in solutions) differs from ideal conditions by the activity coefficient (γ) [37]. Equation 2.11 shows the activity for species i for a solute and gas, respectively.

$$\mathrm{a_i} = \gamma_\mathrm{i}\frac{\mathrm{c_i}}{\mathrm{C^0}} \qquad\qquad \mathrm{a_i} = \gamma_\mathrm{i}\frac{\mathrm{p_i}}{\mathrm{P^0}} \tag{2.11}$$

Here, c_i is the concentration of the solute, C^0 is the standard concentration (~ 1 M), p_i is the partial pressure, and P^0 is standard pressure (1 bar). Activity coefficients are rarely known [38], which yields a motivation to avoid the term completely [29, 39]. One option that is frequently used, is assuming ideal conditions ($\gamma_\mathrm{i} \approx 1$). The ideality approximation is common for gases at atmospheric or lower pressures and ambient or higher temperatures [40]. Combining Equation 2.9 and 2.10, and interchanging activities with partial pressures gives a version of the Nernst equation for gaseous mixes as shown in Equation 2.12

$$E_r = E_r^\circ - \frac{RT}{zF} \ln \left(\frac{p_C^q p_D^r}{p_A^s p_B^t} \right) \tag{2.12}$$

Measuring the actual OCV in a system and comparing it to the theoretical reversible voltage, tells something about how close to its maximum potential the cell can perform, and gives an indication of any presence of undesirable phenomena, such as degraded or destroyed fuel cell materials, reactant losses or insufficient reactant concentrations.

2.3.2 Operational voltage

When a load is connected, cell voltage drops to what can be called operational voltage. This is due to the several irreversibilities, also called overpotentials, listed below [29, 41].

1. **Activation losses** occur at the interfaces between the electrodes and the electrolyte and can be thought of as a resistance to the electrochemical reaction itself. Some voltage is drained to overcome the activation energy for the specific reactions. This overpotential is most often referred to only as "polarisation".

2. **Ohmic losses** are related to resistance to electron flow in the circuit and electrodes, and ion flow through the electrolyte.

3. **Concentration losses** is connected to insufficient transport of reactants. Consumption of reactants at the interface causes a concentration gradient, with insufficient diffusion from the bulk mass to the reaction sites.

4. **Fuel crossover** means the passing of hydrogen or ammonia through the electrolyte and is a phenomenon that mostly occurs in membrane-based fuel cells. When fuel is crossing over to the cathode, it is wasted, and electrons that otherwise would have gone through the circuit are lost. The unit for fuel crossover is therefore given in mA/cm^2 [29, 42].

The operational voltage is given at a specific current density, by subtracting all the overpotentials from the reversible voltage. Even though reversible cell voltage is lowered at elevated temperatures as can be seen in Equation 2.12, operational voltage, on the other hand, increases. This is due to increased kinetics which reduces polarisation losses, and increased ionic conductivity which reduces ohmic losses.

2.3.3 Power density

To compare fuel cells of different sizes, area-specific quantities are practical. Current density is a key parameter in fuel cells with unit mA/cm^2 or current per unit area [29]. Current density is given together with the operating voltage, which multiplied gives the power density in mW/cm^2. When current density increases, power density will also increase until a certain point, where a further increase of current density will lower the cell voltage and power density due to irreversibilities. The maximum power density is referred to as Peak Power Density (PPD). Specific power in kW/kg can also be a useful measure for weight-dependent applications.

2.3.4 PPD ratio

As H_2 is the most prominent fuel for fuel cells, the performance of the fuel cell fed with H_2 is often used as a reference to compare the performance of other fuels in the same system. The PPD ratio is the peak power density of ammonia divided by the peak power density of hydrogen in the same cell under equal conditions, as in Equation 2.13

$$\text{PPDratio} = \frac{\text{PPD}_{\text{NH}_3}}{\text{PPD}_{\text{H}_2}} \times 100(\%) \tag{2.13}$$

2.3.5 Durability

An important aspect when looking towards the commercialisation of fuel cells and stacks is the durability of the cell. A high-performance cell is not viable for commercial applications if it is quickly degraded. Comparing cell life is, however, not straightforward. One suggestion is the number of hours before failure, others use the number of operating hours before the delivered power drops below rated power. As the fuel cell ages, it will experience degradation and decreased ability to deliver sufficient power. Several factors can enhance degradation, for example high temperatures and fuel impurities. For single cells, degradation rates of V/h are often given, and larger scale systems give degradation rates in %/1000 h.

2.3.6 Efficiency

The electrical efficiency of an ammonia fuel cell (AFC) is given by Equation 2.14 [3].

$$\eta_{\mathrm{AFC}} = \frac{\dot{\mathrm{P}}_{\mathrm{out}}}{\dot{\mathrm{N}}_{\mathrm{NH_3}} \overline{\mathrm{LHV}}_{\mathrm{NH_3}}} \tag{2.14}$$

Here, $\dot{\mathrm{P}}_{\mathrm{out}}$ is the delivered power, $\dot{\mathrm{N}}_{\mathrm{NH_3}}$ is the molar flow rate of ammonia fed to the anode, and $\overline{\mathrm{LHV}}_{\mathrm{NH_3}}$ is the molar lower heating value of ammonia. The lower heating value will need to be exchanged with higher heating value for fuel cells operating on low temperatures, where the water stays liquid.

When expanding the system under investigation to a cogeneration system containing several components such as afterburners, turbines, compressors, batteries or engines, the efficiency of each component should be included. The total output power is then divided by the power of the fuel supplied.

Now that we are familiar with the performance metrics for fuel cells, the specific working of the three relevant fuel cell technologies for the review will be described.

2.4 Working of solid oxide fuel cells

Solid oxide fuel cells rely on a solid oxide or *ceramic* electrolyte to conduct ions. For ceramic electrolytes to conduct ions, high operating temperatures (400-1100 °C) are needed. SOFCs can be divided into categories based on which temperature range they operate within. High temperature (HT), intermediate temperature (IT) and low temperature (LT) SOFC operate at around 800-1000 °C, 650-800 °C, and 500-650°C respectively [12]. These high temperatures are an advantage for several reasons. High temperatures make the thermal dissociation of ammonia (see Table 2.2) and other fuels possible, which creates a fuel-flexible device. Also, the high temperature generates an energetically valuable exhaust, that can be further used in Combined Heat and Power (CHP) plants.

2.4.1 Oxide ion conducting solid oxide fuel cells

In SOFC-Os, ammonia is decomposed at the anode, normally in the presence of a nickel catalyst. Oxide ions (O^{2-}) reduced from oxygen at the cathode, migrate through the electrolyte to the anode to form water according to the half-reactions depicted in Figure 2.3. The O^{2-} ions move between oxygen vacancies in the crystal lattice [43]. These vacancies are positions in the crystal lattice where an oxygen atom was originally supposed to be, but instead, doping (see Section 2.4.3) of the material has been done to create voids for ions to move [44].

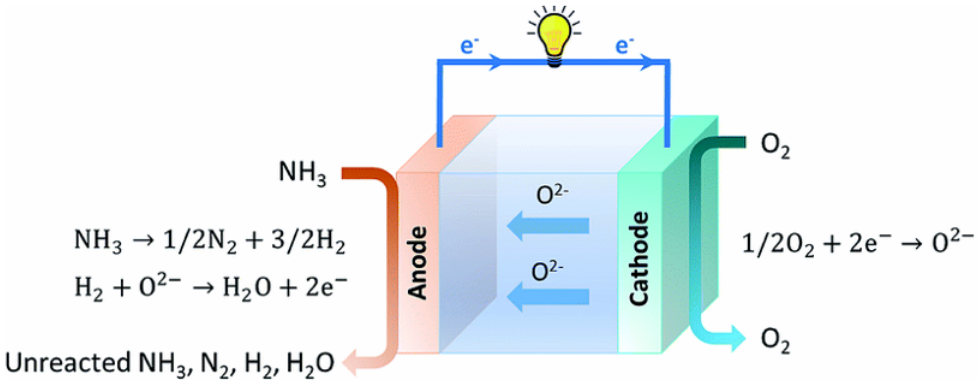

Figure 2.3: Schematic of oxide ion conducting SOFC. Ammonia decomposition and anode- and cathode half-cell reactions are shown. Reprinted from Jeerh et al. [11], open access.

2.4.2 Protonic ceramic fuel cells

In PCFCs, ammonia is decomposed, and the following H_2 is oxidised into protons at the anode and move through the electrolyte. At the cathode, the protons form water with oxygen according to the half-reactions in Equation 2.15 and 2.16, respectively. Figure 2.4 shows a schematic of the PCFC and a detailed view of the anode and cathode processes.

$$H_2 \longrightarrow 2H^+ + 2e^- \tag{2.15}$$

$$\frac{1}{2}O_2 + 2H^+ + 2e^- \longrightarrow H_2O \tag{2.16}$$

As in SOFC-Os, the crystal lattice of the ceramic electrolyte in PCFCs also contains oxygen vacancies, but these vacancies are further incorporated with water to enable proton

conduction through the Grotthus mechanism [45]. After water incorporation, the oxygen atoms in the water molecules are stationary in the former oxygen vacancies. The associated protons can now hop between neighbouring water molecules, leaving a spot behind for another proton to occupy temporarily, and so the migration goes forward. To enable proton conduction, some amount of water in the fuel mix is beneficial in PCFCs [16].

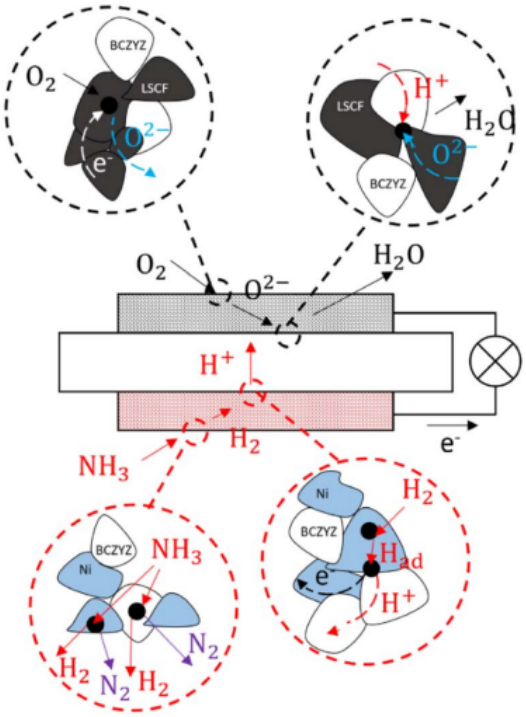

Figure 2.4: Schematic of PCFC fed with ammonia with a BCZYZ ($BaCe_{0.7}Zr_{0.1}Y_{0.16}Zn_{0.04}O_{3-\delta}$) electrolyte, Lanthanum Strontium Cobalt Ferrite (LSCF)-BCZYZ cathode (top) and Ni-BCZYZ anode (bottom). NH_3 is decomposed at the outer anode surface, and H_2 diffuses towards the TPB where it is oxidised and releases electrons. At the cathode, O^{2-} diffuses from the surface and forms water at the cathode TPB with the incoming protons. Reprinted from Nowicki et al. [46], open access.

2.4.3 SOFC materials

Most materials seen in solid oxide fuel cells (PCFC and SOFC-O) are either fluorite or perovskite structured [47]. Fluorites are cubic structures with the general formula MX_2, where M denotes a large four-valent cation, and X is an anion, often oxygen, creating oxides in the case of SOFC [48].

The widely used SOFC-O electrolyte Yttria-stabilised Zirconia (YSZ) for example, consists of a fluorite-structured oxide, namely zirconium dioxide, also called zirconia (ZrO_2), doped with yttrium oxide (yttria, Y_2O_3). Zirconia alone is a poor ionic conductor with

a monoclinic structure at room temperature, but when heated above 2370°C, changes its crystalline structure to a cubic fluorite structure, which enables ion conduction [29]. The yttria is introduced to stabilise the structure, to obtain the cubic form at lower temperatures and also to create oxygen vacancies for ions to move (see Figure 2.5). YSZ is very dense, making an excellent barrier between the reactants, and is chemically inert under a wide range of conditions.

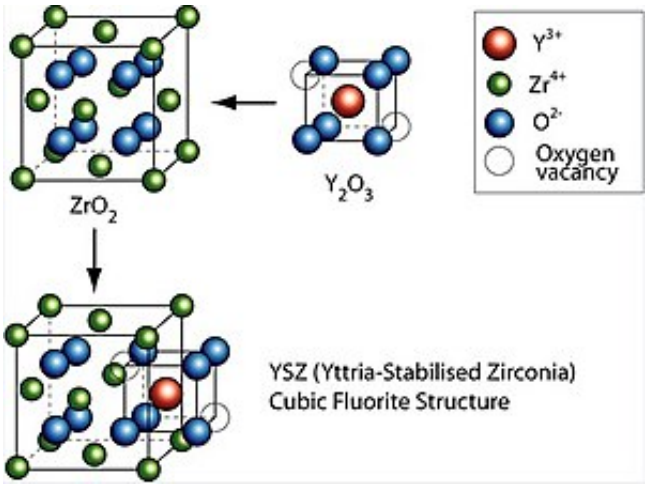

Figure 2.5: Yttria is incorporated into zirconia to create the O^{2-} conducting yttria-stabilised zirconia. Reprinted with permission [29].

Simple perovskites have the general formula ABO_3, where A and B are cations. A are often larger rare-earth cations like yttrium, scandium or lanthanoids, or alkaline-earth cations such as magnesium, strontium or barium [29]. The B-site cations are usually transition metal elements like lanthanum and zirconium [29]. Perovskites are often seen as electrodes in SOFC, as many perovskites are Mixed Ionic Electronic Conductors (MIECs). An example is the much-used cathode material Lanthanum Strontium Manganite (LSM). Here the A-sites are lanthanum mainly, but some lanthanum sites are substituted (doped) with strontium, and the B-sites are manganese cations, making out the chemical formula $La_{1-x}Sr_xMnO_3$. By varying the choices for A and B cations, and the amount of dopant (x), there are practically speaking endless options for material configurations with different applications and physical properties [49].

Single fuel cells are, as we know, primarily built up by the electrolyte sandwiched between the anode and the cathode. However, one could further divide the anode and cathode into functional layers and support layers. The functional layer is often limited to the part of the electrode which is closest to the electrolyte, while the support layer is where

the diffusion and decomposition of ammonia occurs. Depending on which layer (anode, electrolyte, cathode) is the thickest, the cell is said to be supported by that layer. So in an anode-supported cell, the anode stands for the mechanical stability of the cell. The materials of the fuel cell are usually stated in this form; anode|electrolyte|cathode, which for a conventional SOFC-O with LSM cathode, YSZ electrolyte and Ni-YSZ anode corresponds to Ni-YSZ|YSZ|LSM.

2.5 Working of anion exchange membrane fuel cell

In anion exchange membrane fuel cells, humidified ammonia gas or aqueous ammonia solution is input at the anode. Here, NH_3 reacts electrochemically with hydroxyl ions (OH^-) to emit electrons and form nitrogen and water, as shown previously in Equation 2.8 and Table 2.3. The anodic and cathodic half-cell reactions are given in Equation 2.17 and 2.18, respectively.

$$2NH_3 + 6OH^- \longrightarrow N_2 + 6H_2O + 6e \tag{2.17}$$

$$\frac{3}{2}O_2 + 3H_2O + 6e \longrightarrow 6OH^- \tag{2.18}$$

The fuel cell is built up by a solid semipermeable polymer membrane, normally accompanied by carbon-supported electrodes with platinum-based catalysts as demonstrated in Figure 2.6. The technology is much similar to PEMFC but can be regarded as the inverse of PEM technology. Here OH^- ions migrate through a modified polysulfone membrane treated with a KOH solution, by moving between hydroxide conducting functional groups (Quaternary Ammonium (QA)) [50]. Polysulfone is a robust and thermally stable polymer up to 200°C, but operating temperatures for AEMFC are normally around 50-100°C to avoid membrane damage [51]. The advantages of these fuel cells compared to traditional aqueous alkaline fuel cells are the removed risk of electrolyte leakages as well as the possibility of more compact designs, leading to higher power densities.

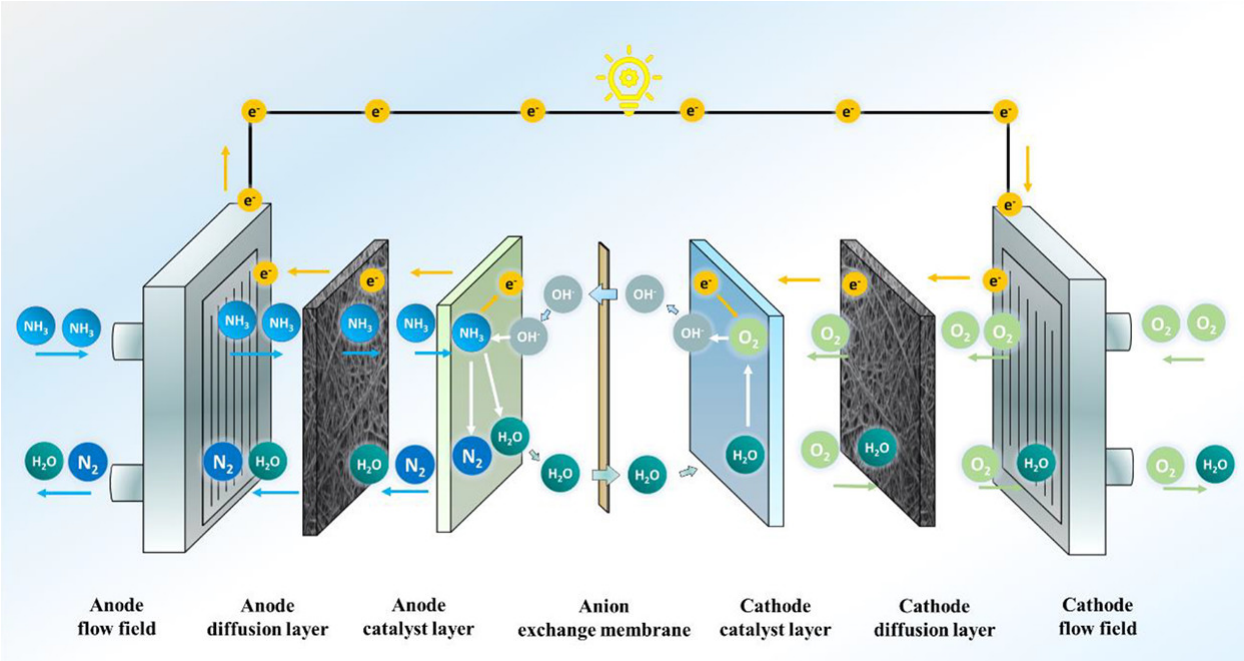

Figure 2.6: Schematic of the build-up and working of a NH_3-fed AEMFC. The diffusion layers ensure an even distribution of fuel/oxidant to the electrodes. Reproduced with permission [52].

In-depth descriptions of the properties of different commercial anion exchange membranes utilised in the AEMFCs in the following review will not be given, and falls outside the scope of the thesis. Rather, a general example of AEM properties is presented here to form a basis for understanding the membrane working. AEMs are between 25-50 μm thick and have an OH^-conductivity of between 15-80 mS/cm and water content at around 25 wt% [53, 54]. The now well-known SOFC-O YSZ electrolyte has a conductivity of 20 mS/cm at 800°C, as a reference [29].

CHAPTER 3

Review and discussion

3.1 Oxide ion conducting solid oxide fuel cells

Historically, two important pieces of work stand out as groundbreaking for the advancement from SOFC developed for hydrogen and hydrocarbons mainly, to ammonia fuel cells. The first is Vayenas and Farr's experiments in 1980 [55, 56], where ammonia was fed to a SOFC with Pt electrodes and a 2 mm thick YSZ electrolyte with the purpose of co-producing nitric oxide (NO) and electricity. They stated that in temperatures of between 900-1200 K, the selectivity towards NO was promising, but lower and higher temperatures, however, mainly yielded N_2. The second is Wojcik et al.'s [57] trials as the first where ammonia was solely intended for energy purposes. Here, tubular SOFC-O with YSZ electrolyte was tested with several anode materials, including silver and platinum, with and without iron catalysts at different temperatures. They showed that ammonia gave similar power outputs as with H_2 and affirmed ammonia as a promising direct fuel for electricity generation in SOFC.

3.1.1 Recent progress

Conventional SOFC-O materials include YSZ electrolyte, LSM cathode and nickel-based anodes, usually Ni-YSZ. In 2006, Ma et al. [58] executed experiments with ammonia fed to a fuel cell comprising these materials, but with a thin-film electrolyte of 30 μm. They achieved a PPD of 526 mW/cm^2 at 850°C, only slightly lower than when fuelled with H_2 at the same temperature. At lower temperatures, the ammonia decomposition was

not sufficient and the authors stated that, for the mentioned fuel cell, ammonia was only suitable as a direct fuel at temperatures above 750°C. In 2012, Zhou et al. [59] proved that ammonia could achieve equal PPDs as hydrogen in a SOFC with Fe-infiltrated SSZ. The study stands out as the only one with a cell performing slightly better with NH_3 than H_2.

Until recently, Meng et al.'s [60] reported PPD of 1190 mW/cm^2 in 2007 has been regarded as the state-of-the-art performance of ammonia-fed SOFC-O. The fuel cell tested comprised a 10 μm-thick Samarium-doped Ceria (SDC) electrolyte, Barium Strontium Cobalt Ferrite (BSCF) cathode and NiO anode. However, several studies have surpassed these PPD values in the last year, reporting PPDs as high as 1893 mW/cm^2 [61], which is, to the best of knowledge, the highest PPD for DA-SOFC-Os reported to date. A selection of SOFC-Os tested are presented in Table 3.1, with an emphasis on the most recent achievements.

Table 3.1: A selection of NH_3/air-fed SOFC-Os reported in literature, and their performances.

Anode/ cathode	Electrolyte	Electrolyte thickness (μm)	Temp. (°C)	Peak power density (mW/cm^2)	OCV	PPD-ratio (%)	Reference/ year
NiO-YSZ/LSM	YSZ	30	650 750 850	86 299 526	1.08 1.07 1.03	91.5 98 99.2	[58]/2007
NiO/BSCF	SDC	10	550 600 650	167 434 1190	0.795 0.771 0.768	22.3 31.9 63.5	[60]/ 2007
Fe infiltrated Ni-SSZ/SSZ-LSM	SSZ	15	700 750 800	455 735 1150	1.12 1.11 1.10	101.3 102 98.2	[59]/2012
Ni-NCAL/Ni-NCAL	SDC/NCAL	∼ 748	450 500 550	153 501 755	0.87	45.8 74.7 84.3	[62]/2022
Ni-Al_2O_3-YSZ/LSCF	YSZ	8-10	650 700 750	81* 121* 204*		79.3 88.3 97	[63]/2022
Ni-GDC/unknown	GDC-YSZ-GDC	∼ 2 (18-2-18)	550 600 650	342 557 1330	1.09 1.10 1.11	28.0 35.1 67.8	[64]/ 2022
Ni-YSZ/PBCC	YSZ	8	700 750 800	673 997 1375		 86.2	[61]/ 2023
$CeO_{2-\delta}$infiltrated Ni-YSZ/PBCC	YSZ	8	700 750 800	941 1351 1893		 88.3	[61]/2023

BSCF: $Ba_{0.5}Sr_{0.5}Co_{0.8}Fe_{0.2}O_{3-\delta}$, LSM: $Ce_{0.8}Sm_{0.2}O_{2-\delta}$, SSZ: $Sc_{0.1}Zr_{0.9}O_{1.95}$, NCAL: $LiNi_{0.815}Co_{0.15}Al_{0.035}O_2$, SDC: $Sm_{0.2}Ce_{0.8}O_{2-\delta}$, LSCF: $La_{0.6}Sr_{0.4}Co_{0.2}Fe_{0.8}O_{3-\delta}$, GDC: $Gd_{0.1}Ce_{0.9}O_{2-\delta}$, PBCC: $PrBa_{0.8}Ca_{0.2}Co_2O_{6-\delta}$
*: power density at operational voltage 0.85 V, not PPD.

As Table 3.1 shows, both Xu et al. [61] and Oh et al. [64] have reported higher PPDs than Meng et al. [60]. Oh et al. [64] attained this PPD at the same operating temperatures as Meng et al. (650 °C), as opposed to Xu et al.'s [61] record result at >750 °C. When, on the other hand, the temperatures were lowered in the $CeO_{2-\delta}$ infiltrated cell, the performances were clearly inferior to both Oh et al. [65] and Meng et al.'s [60] cells. Nevertheless, the results of Xu et al. [61] are still promising, as other valuable characteristics were seen. The infiltration of nano-sized $CeO_{2-\delta}$ particles improved cell durability compared to the bare anode, and also enhanced the ammonia decomposition activity. Several factors were listed as the reason for the favourable effect of $CeO_{2-\delta}$, such as a stabilising effect on the nickel particles, where $CeO_{2-\delta}$ worked as a protective layer against NH_3 exposure to the anode. Also, the nano-particles were stated to extend the TPB, which created more active sites for NH_3 decomposition.

The choice by Oh et al. [64] to sandwich a very thin layer of the ion-conducting YSZ between Gadolinia-doped Ceria (GDC) stems from the higher ionic conductivity of doped ceria, compared to YSZ [65]. However, YSZ is used because it is a denser and pure ionic conductor compared to the mixed ionic-electronic GDC [65]. With only 2 μm of the dense YSZ, ohmic losses are minimised. In the same work, comparisons were made between this novel high-performance cell and two others, a commercial bulk Ni-YSZ|YSZ|Lanthanum Strontium Cobalt (LSC) cell, and a thin-film (TF) cell with the same materials [64]. The results are reproduced in Figure 3.1. It can be seen in Figure 3.1A,B,C and E, that the bulk-Ni/YSZ cell had a very small performance gap between H_2 and NH_3 at all temperatures, even though performances, in general, were very low compared to both thin-film cells. Up till 600°C, the TF-Ni/YSZ and TF-Ni/GDC cells performed almost identically when fuelled with NH_3, but at 650 °C, the Ni/GDC cell clearly performs better (Fig 3.1D). However, the difference between the NH_3 and H_2 performance is significant. The authors ascribed the differences to the insufficient NH_3 decomposition activity and gas transport.

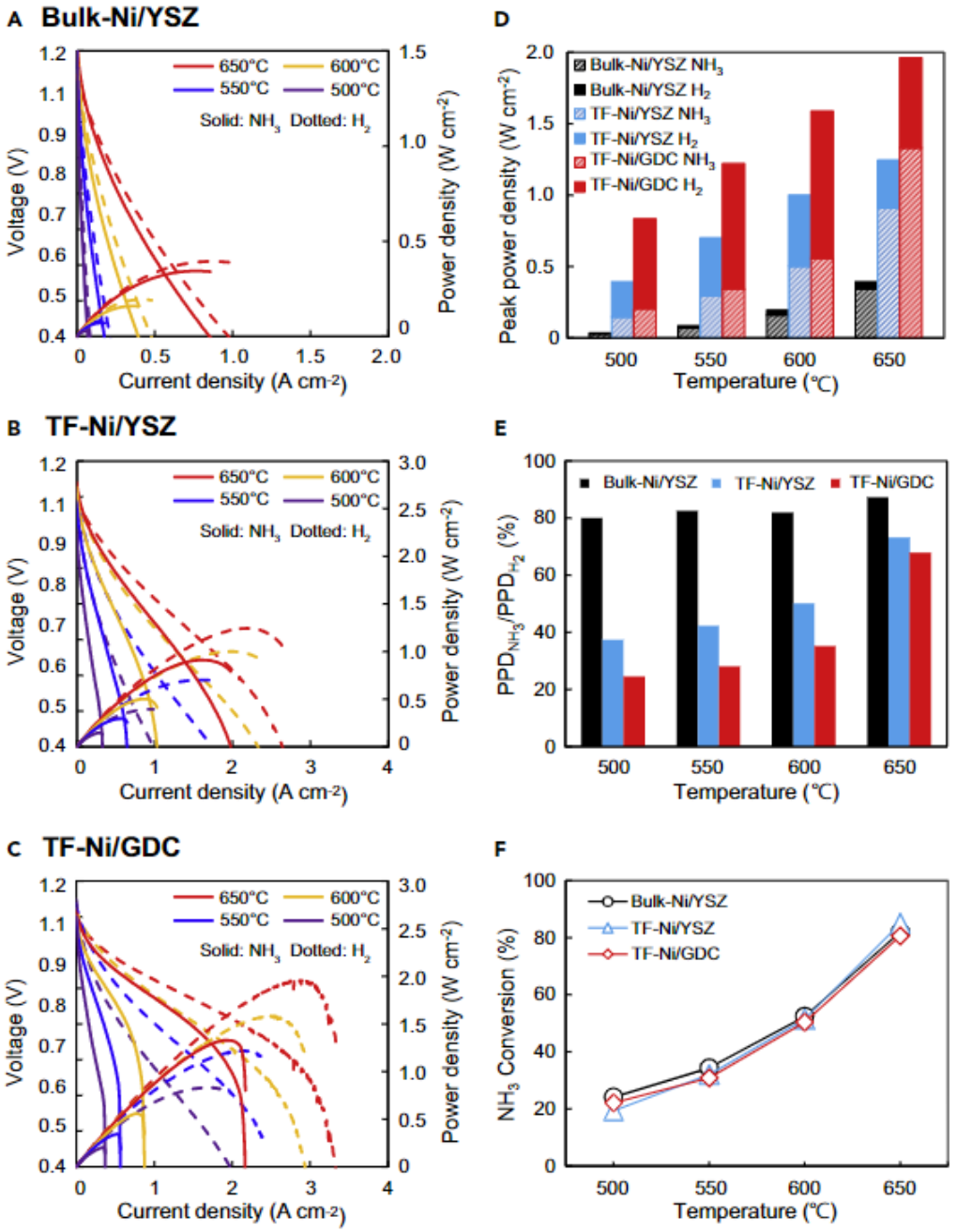

Figure 3.1: A, B and C show the voltages and power densities for three different fuel cells operated at different temperatures and current densities with NH_3 and H_2 fuel. D and E compare PPDs between the cells and the fuels, and F shows NH_3 conversion rate for the three cells. Reprinted from Oh et al. [64], open access.

The results reported by Quian et al. [62] show surprisingly great potential also at lower temperatures for SOFC-O. A symmetrical cell with Ni-$LiNi_{0.815}Co_{0.15}Al_{0.035}O_2$ (NCAL) for both electrodes was designed, with an SDC/NCAL (70:30) electrolyte, and was reported to achieve relatively high PPD and PPD-ratio. Doped ceria has good ionic conductivity at lower temperatures, and NCAL ($LiNi_{0.815}Co_{0.15}Al_{0.035}O_2$), which is a composite

semiconductor material, entails both ionic and electronic conductivity that increases the TPB [66]. Using the same material for the cathode and anode in a symmetrical setup makes fabrication cheaper and easier and ensures a higher degree of mechanical compatibility between the cell components. The use of semiconductors as electrolytes in SOFC is a relatively new concept and involves the utilisation of the different materials' interfacial band gap energy as an electron blockage to prevent short-circuiting through the electrolyte [67]. Higher PPDs than the reported 755 mW/cm^2 have not been described previously at this temperature for ammonia fuel cells, and the mentioned cell can provide a promising new alternative for low-temperature DA-SOFC-Os if the durability of these materials also can be proven.

3.1.2 Durability

Within 2020, the U.S. Department of Energy (DOE) aimed to meet SOFC degradation rate targets of no more than 0.2%/1000h and simultaneous cell life of at least 40 000 hours [68]. These targets applied to commercial hydrogen and hydrocarbon SOFC-O stacks. Experts, however, anticipated this goal to be reached in 2050. As DA-SOFC is a newer technology, the degradation rates are expected to be slightly higher.

Properly pre-dissociated ammonia is shown to provide no more degradation than what H_2-fed systems already experience [69, 70]. Golkhatmi et al. [71] reviewed the main degrading mechanisms for SOFC, and ascribed cathode degradation mainly to poisoning by chromium from unprotected metallic interconnects, as well as CO_2 and sulfur poisoning from the air. Even if the content of these is at ppm-scale in air, it can still affect cell performance [71]. For the electrolyte, phase transitions of the crystalline structure, as well as chemical interactions with the electrodes, especially the cathode, were mentioned as the most salient degradation mechanisms. For all components, thermal stress at high operating temperatures can cause mechanical failure, especially after several cycles of heating and cooling the stack.

Direct ammonia-specific degradation is limited to the anode and is mainly caused by nitriding [62, 72]. In high-temperature ammonia atmospheres, nickel particles are prone to agglomerate and form Ni_3N, which coarsens the otherwise porous anode. Yang et al. [73] reported that nitriding especially occurred at lower temperatures (<600 °C), as the

ammonia decomposition decreased. When temperatures were elevated, Ni_3N was reduced back to Ni again. A thermal cycle test was conducted, and OCV was observed to drop significantly as seen in Figure 3.2. Also, when investigating the anode after the test, a crack was found in the anode support layer as a result of the repeated nitriding cycles. Ensuring prompt and close to 100% ammonia decomposition when the fuel enters the anode is crucial to prevent nitriding degradation. This can be challenging as the trend is moving towards lower operating temperatures, which compromises the thermal ammonia cracking and increases the reliance on effective ADR catalysts.

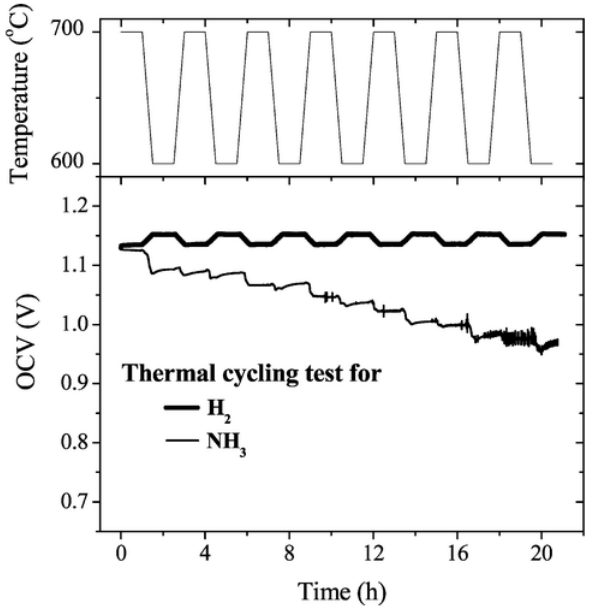

Figure 3.2: Degradation of a fuel cell fed with NH_3 and H_2 during a thermal cycling test. Reprinted from Yang et al. [73], open access .

Few long-term stability tests have been run on cell-level, but shorter tests of around 100 h are more frequently reported. Xu et al. [61] ran a 60 h test at their high-performing cell (see Table 3.1) at a current density and temperature of 0.5 A/cm^2 and 700°C, respectively. The test yielded a degradation rate of 0.127%/h. Amongst longer-term stability tests on cell level is Hagen et al.'s [70] experiments with a commercial Ni-YSZ|YSZ|LSM-YSZ SOFC tested with ammonia and biogas. Figure 3.3a shows a comparison of cell voltage and power density for the cell fed with NH_3 and an equivalent mix of H_2/N_2. The curves are almost overlapping, indicating very sufficient internal NH_3 decomposition. Further, Figure 3.3b shows the electrical efficiency and power output during a durability test. A 2-4%/1000 h degradation was reported, compared to only 1%/1000h for biogas in the same system. The electrical efficiency of around 40% is somewhat lower than the 50-60%

efficiency that SOFCs often are claimed to have [74]. In comparison, the biogas fuel cell had a 47% electric efficiency at a lower temperature (750 °C), but in a slightly modified cell. These results clearly show that ammonia has a way to go compared to the more extensively used hydrocarbons.

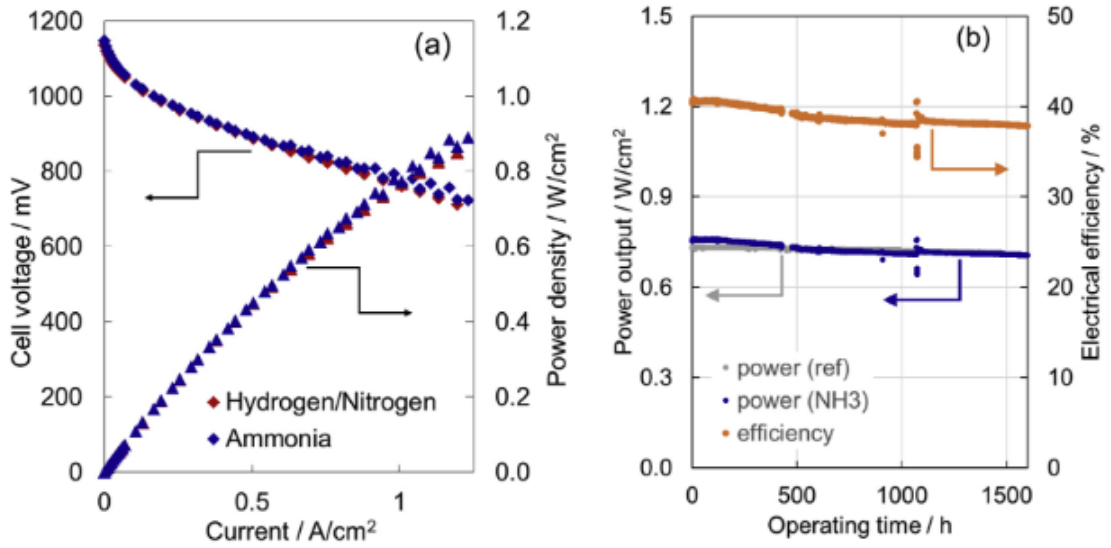

Figure 3.3: (a) shows cell voltage and power density at different current densities for a Ni-YSZ|YSZ|LSM-YSZ cell tested in ammonia and an equivalent hydrogen/nitrogen mix. (b) shows efficiency (orange) and power output (blue) during a 1500 h durability test executed at 850 °C and current density 1 A/cm^2. The grey curve is a reference curve based on H_2 fuel feed. Reprinted from Hagen et al. [70], open access.

Golkhatmi et al. [71] stated that "most SOFCs that perform well do not possess good stability", which is important to remember when attempting to compare fuel cells. While increased operating temperatures and thin layers of materials improve cell performance, it also makes the cell fragile and prone to mechanical failure. Balancing performance and durability has proven difficult, but is crucial to enable SOFC commercialisation.

3.1.3 Systems and large-scale stacks

Few experimentally tested DA-SOFC-Os at system level are found in the literature, and modelling studies mostly describe the indirect use of ammonia, but some also entail DA-SOFC-O [75–77]. One of the earliest reported models based on experimental tests is Cinti et al.'s [78] test with a four-cell short-stack. The stack had a Ni-YSZ|YSZ(10μm)|YSZ-LSM configuration and was tested with three different fuel configurations; pure NH_3, a stoichiometrically equivalent mix of N_2/H_2, and H_2. It was stated that the endothermic nature of ammonia decomposition was an advantage from a thermodynamic point of view,

as no additional cooling was needed for the stack. This would yield a 22% increase in electrical efficiency compared to when fuelled with H_2. The model also showed that a stack fed with pure ammonia would perform almost equal to the stoichiometrically equivalent N_2/H_2-mixture. These latter results were confirmed experimentally by Kishimoto et al. and Hagen et al..

Kishimoto et al. [10] first tested a 200 W stack [79], before they further developed a 1 kW DA-SOFC-O stack that they tested both alone and with an external cracker. The stack consisted of 30 planar anode-supported cells with Ni/YSZ anode, a ZrO_2-based electrolyte and a perovskite cathode. The stack yielded an efficiency of 52% at 1 kW power output. Compared to the one fuelled with H_2-N_2-mixture, the latter performed slightly better at high currents. Such a minimal gain suggests that external crackers are in excess when it comes to fuel cell performance, and will cause additional cost and spatial needs. However, external crackers are useful for increased durability, as nitriding is not an issue. The 200 W stack was reported to have a degradation rate of 5%/1000h when fed with NH_3 for 1000 h at ∼700°C. The 1 kW stack was stated to have no signs of degradation after a similar durability test. However, it could be seen that the average cell voltage was slightly higher and less fluctuating when ammonia was pre-decomposed compared to when fed directly to the anode during the durability test (see Figure 3.4). This can be ascribed to the more stable temperature at the anode, as the endothermic ammonia cracking occurs outside the fuel cell.

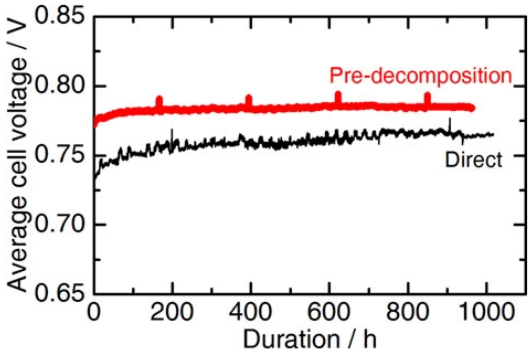

Figure 3.4: Cell voltage over time during a 1000 h durability test for pre-decomposed NH_3 (red), compared to direct NH_3 feed (black). Reprinted from Kishimoto et al. [10], open access.

The stack in this experiment was kept inside a furnace to keep temperatures up. As stacks are scaled up, utilising the heat balancing between the endothermic ammonia cracking and the exothermic hydrogen oxidation may provide an increase in system efficiency as Cinti et al. [78] reported in their theoretical study. Few articles touch upon this topic to date.

Stoeckl et al. [80] developed a wastewater energy recovery system where a 10-cell commercial stack was tested. The fuel cells had a Ni-GDC|Scandia-stabilised Zirconia (SSZ)|LSM-SSZ configuration. The system was fed with a 70% ammonia 30% steam mix, as this was the expected output mix from the wastewater distillation. A durability test of 1000 h was also conducted, and during this time span the power density decreased from 181 mW/cm^2 to 179 mW/cm^2, which corresponded to a degradation rate of 1.1%/1000h. An analysis after the test showed nitriding in the interconnects, which was stated to be the main reason for performance degradation. No significant changes were observed in the anode functional layers. The analysis of the exhaust showed that the ammonia decomposition rate was 99.98%. Such high ammonia decomposition contributed to the minimal performance differences between NH_3 and equivalent N_2/H_2 fuel feed.

An ongoing scale-up project utilising direct-ammonia SOFC is the ShipFC project, where zero-emission deep-sea shipping is planned to be demonstrated in 2025 [81]. Here, a 2 MW DA-SOFC-O system will be integrated together with two already installed dual-fuel engines, capable of running on ammonia. Alma Clean Power is currently developing the system and states that it will provide a 60% efficiency [74].

3.2 Protonic ceramic fuel cells

In recent years, PCFCs have gained momentum for many reasons. Theoretically, OCV and thereby power output should be higher than for SOFC-O due to the higher fuel concentrations at the anode since water is formed at the cathode, hence preventing fuel dilution. Moreover, lower polarisation losses are expected in PCFC due to the more facile transport of H^+ compared to that of the larger O^{2-} [82]. Also, ion conduction occurs at lower operating temperatures, which can help mitigate thermal stress and degradation.

Iwahara et al. [83] conducted a series of experiments in the 1980s on doped barium cerate perovskites for proton conduction, and are regarded as pioneers within proton conducting oxides [45]. Doped barium cerates are still widely used for PCFC electrolytes and electrodes, with several dopants and configurations tested. However, emerging as a more popular option recently is barium zirconates [84]. The most common PCFC material seen today is configurations of ceria and Yttria-doped Barium Zirconate (BZCY). The order of the letters points to which element is in abundance. So BCZY will, in general, have a higher amount of cerium compared to BZCY. Barium zirconate has fast proton diffusion and is more stable in CO_2 and steam atmospheres, also at lower temperatures, compared to the more traditional barium cerate [85]. Increased amounts of cerium enable even better protonic conductivity, while Zr provides stability [84, 85]. Trade-offs between the two are made based on applications and operating conditions.

Cathode processes for PCFC differ from SOFC-O, due to the water formation here, which makes stability against steam gas an important additional cathode property [86]. The popular mixed ionic-electronic conducting cathode materials BSCF and LSCF are valuable in the more complex cathode reactions occurring in the PCFC. As O^{2-}, H^+ and e^- are all present in the cathode oxygen reduction and water formation reactions, an extension of MIECs, namely triple-conducting cathode materials has been developed by modifying the BSCF cathode [87]. Ensuring sufficient transportation of all of the species increases the triple-phase boundary at the cathode, hence improving the cathode reaction kinetics. To the author's knowledge, triple-conducting materials are not tested in DA-PCFCs, but have been reported with success in H_2-PCFC [87].

3.2.1 Recent progress

A selection of PCFCs is displayed in Table 3.2, also with an enhanced focus on newer articles. As can be seen, palladium (Pd) has been reported both in anode and electrolyte. Aoki et al. [88] tested a pure Pd anode with otherwise conventional electrolyte and cathode materials. The electrolyte was very thin, but this fact was not reflected in the achieved power density. However, without nickel, the typical anode susceptibility of nitriding is avoided. Jeong et al. [89] compared the effects of Pd-infiltration into a porous Yttrium- and Ytterbium-doped Barium-zirconium-cerate (BZCYYb) anode vs an untreated anode, with the goal of achieving a more active and durable ammonia decomposition catalysis.

The effect of Pd-infiltration was reported to be increased activity towards ammonia decomposition as well as reduced polarisation resistance of 70% when compared to the bare anode at 500°C.

Table 3.2: A selection of ammonia/air-fed PCFCs and their performances.

Anode/ cathode	Electrolyte	Electrolyte thickness (µm)	Temp. (°C)	OCV	Peak power density (mW/cm^2)	PPD-ratio (%)	Reference/ year
Ni-CGO/ BSCFO-CGO	BCGO	30	600 650	1.12 1.10	147 200	85.4 89.7	[90]/2007
Pd/LSCF	BZCY	1	500 550 600	1.03 1.00 0.95	210 340 580	87.5 69.4 71.6	[88]/2018
Ni-BZCYYbPd/ BCFZY	BZCYYbPd	17	550 600 650		369 509 724	81 75.5 77	[91]/2021
Fe-decorated Ni-BZCYYb/ PBSCF	BZCYYb	7	550 600 650 700	1.02 1.03 1.01 0.99	360 723 1257 1609	 78	[92]/2022
Fe-layered Ni-BZCYYb/ PB-SCF	BZCYYb	8	600 650 700	1.01 1.01 0.99	327 685 1078	42.1 59 71.5	[93] 2022
Pd-infiltrated NiO-BZCYYb/ PBSCF	BZCYYb	~ 10	500 550 600		345 613 851		[89]/2023
Ni-BCZYZ/ LSCF	BCZYZ	40	750		236		[46]/2023

CGO: $Ce_{0.8}Gd_{0.2}O_{1.9}$, BSCFO: $Ba_{0.5}Sr_{0.5}Co_{0.8}Fe_{0.2}O_{3-\delta}$, BCGO: $BaCe_{0.8}Gd_{0.2}O_{3-\delta}$, LSCF:$La_{0.6}Sr_{0.4}Fe_{0.8}Co_{0.2}O_3$, BZCY: $BaZr_{0.1}Ce_{0.7}Y_{0.2}O_{3-\delta}$, BZCYYbPd: $Ba(Zr_{0.1}Ce_{0.7}Y_{0.1}Yb_{0.1})_{0.95}Pd_{0.05}O_{3-\delta}$, BCFZY: $BaCo_{0.4}Fe_{0.4}Zr_{0.1}Y_{0.1}O_{3-\delta}$, BZCYYb: $BaZr_{0.1}Ce_{0.7}Y_{0.1}Yb_{0.1}O_3$ PBSCF: $PrBa_{0.5}Sr_{0.5}Co_{1.5}Fe_{0.5}O_{5+\delta}$, BCZYZ: $BaCe_{0.7}Zr_{0.1}Y_{0.16}Zn_{0.04}O_{3-\delta}$

He et al. [91] used the Pd-doped BZCYYbPd both as anode and electrolyte material, which was stated to provide enhanced proton conductivity. Pd nanoparticles were dispersed on the surface of the perovskite anode, which lead to increased ammonia decomposition between 500-600 °C compared to the bare anode. A possible explanation for the increased ammonia decomposition was suggested to be a more facile N_2 recombination facilitated by Pd. Even though the amount of Pd was very small, noble materials are rare and expensive, which might be a problem when scaling up. Iron is, on the other hand, an abundant and cheap metal that has shown superior performance. Zhang et al. [92] recently reported the highest PPD of 1609 and 1257 mW/cm^2 at 700°C and 650°C, respectively, which is similar to SOFC-O performances at the same temperatures. This was done in a planar cell with a Fe-decorated Ni-BZCYYb anode. The infiltration of Fe created a FeNi alloy that reduced the polarisation resistance, due to increased ammonia decomposition kinetics. A 100 h stability test at 650°C was also conducted, where the degradation rate of the NH_3-fed cell was similar to the one fed with H_2.

Two other configurations of Fe with the same Ni-BZCYYb anode were also published in 2022. First Pan et al. [93] tested similar materials in a tubular cell, but with an internal catalyst layer of pure Fe printed onto the Ni-BZCYYb anode support layer. The cell achieved a PPD of 1078 mW/cm^2 at 700°C, which was superior to the bare anode. The configuration can be seen in Figure 3.5. Moreover, the Fe layer worked as as a protective layer of the nickel, preventing nickel nitriding.

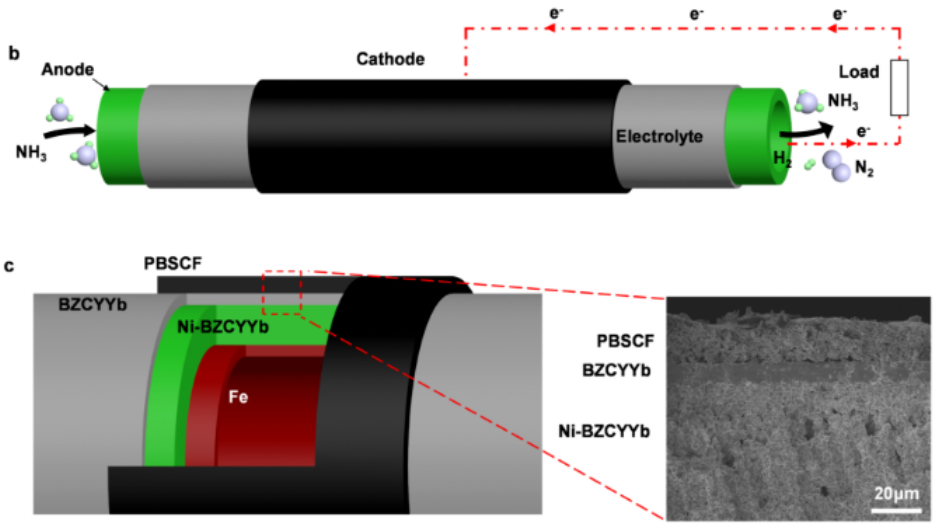

Figure 3.5: Tubular PCFC with internal catalyst layer. Reprinted from Pan et al. [93], open access.

Later, Chen et al. [94] tested an identical cell but with a slight modification to the Fe-layer, namely a Fe-CeO_x and achieved somewhat lower PPD of ∼1060 mW/cm^2 at 700°C. Fe-CeO_2 was, however, stated to increase stability and ammonia conversion compared to the bare anodes with Fe only, due to less agglomeration caused by iron nitriding, which was seen at lower temperatures. As with nickel nitriding, iron nitriding decreases porosity, which is crucial to maintain to ensure sufficient active area for ammonia decomposition.

Nowicki et al. [46] developed and tested a tubular fuel cell for maritime applications. The single cell generated up to 8.5 W at 750 °C. The electrolyte was slightly doped with 4% zinc as a sintering aid. The reason for this doping stemmed from a concern about the scale-up of PCFC. The densification temperatures of barium cerates are very high (∼1500 °C [95]), which leads to an expensive and difficult manufacturing process. Moreover, at these temperatures, barium evaporation issues arise. Zinc was therefore stated as a possible solution to lessen these problems, by reducing the sintering temperature.

3.2.2 Systems and durability

PCFCs have not yet been scaled up for ammonia but kW-scale has been demonstrated with hydrogen [96]. However, the indirect use of ammonia is described in smaller systems. One is a button-sized PCFC that was coupled to an external novel Ru-$(BaO)_2(CaO)(Al_2O)$ reversible ammonia catalyst [69]. Here, the system was reported to be able to switch between generating power in fuel cell mode and synthesising ammonia from H_2O and excess H_2/N_2. The fuel cell achieved a PPD of 877 mW/cm^2 at 650°C. In fuel production mode, ammonia production rates reached 1.2×10^{-8} mol NH_3/s cm^2 at ambient pressure. Combining fuel cells and electrolysers, or, more compactly, having them both in one reversible device, is highly relevant as the share of the energy mix relying on fluctuating energy sources like wind and solar is ever-increasing. However, these devices would mostly be relevant at large scale, making Ru-based catalysts impracticable for the purpose, as it is a rare and expensive material.

Few studies have executed long-term durability tests for PCFC, but like SOFC-O, stability is a challenge for PCFC too. Anode issues with nitriding are, as we know, a problem at decreased temperatures, which makes this issue even more relevant for PCFCs that, generally, operate at lower temperatures than SOFC-O. Developing highly active ADR catalysis is therefore crucial. Jeong et al. [89] and He et al. [89] (Table 3.2) both reduced the degradation rate by using Pd in the anode, where the dispersed Pd particles worked as a protective layer for the nickel and hence prevented nitriding. Jeoung et al. reported a decrease from 17% performance degradation with bare BZCYYb to only 2% in the Pd-treated sample after a 100 h test at 500 °C. For the untreated sample, cracks and gas leakage was observed after the test, while the electrolyte still remained in its ideal form in the Pd-treated sample.

Xiong et al. [97] improved durability by slight ruthenium doping a SOFC anode into a $Pr_{0.6}Sr_{0.4}Co_{0.2}Fe_{0.75}Ru_{0.05}O_{3-\delta}$ (PSCFRu) composition. The cell had a $BaCo_{0.4}Fe_{0.4}$-$Zr_{0.1}Y_{0.1}O_{3-\delta}$ (BCFZY) electrolyte and SDC cathode. The configuration of this cell is rather unique, with a PSCF-based anode, which is seen mostly as a cathode material otherwise. It is unclear from the paper whether the cell is proton or oxide-ion-conducting, but based on the electrolyte it is assumed to be proton-conducting. In any case, the anode showed high ammonia decomposition activity, and also high stability of the decomposi-

tion through a 244-hour test executed at 700°C and current density 100 mA/cm^2. For comparison, a similar cell without doping and one with a Ni-SDC anode was tested under the same conditions. The Ru-doped cell was reported to show superior durability with a degradation rate of 0.00047 V/h compared to 0.0056 V/h and 0.051 V/h for the bare PSCF and SDC anode, respectively. The OCV was not given, but by assuming it is ~ 1 V, and that the degradation continues in a linear manner, this corresponds to a degradation rate of 4.7%/1000 h, which is far away from the DOE targets of 0.2% / 1000h, but on the other hand similar to the degradation rates reported in DA-SOFC-O. As PCFCs are a newer and less developed technology compared to SOFC-Os, these similar results are very promising for the further development of ammonia-fed PCFCs.

3.3 Ammonia-specific challenges in SOFC

3.3.1 Ammonia decomposition

Unlike H_2-fed SOFC, where the rate-limiting part of the fuel cell is ascribed to the slow ORR at the cathode [98], the main challenge for DA-SOFC is to ensure sufficient and stable anode kinetics [99]. As a consequence, the preponderance of articles within DA-SOFC research is directed towards anode materials and catalysts.

Ammonia decomposition in the presence of a Ni-catalyst is well proven to approach $\sim$ 100% at above 700°C in conventional YSZ-cells [16]. But as undesirable effects such as degradation and long startup times are following at high temperatures, lower temperatures are wanted. However, at temperatures below 600-700°C, nickel nitride is more stable, and rapid decomposing of ammonia before it reaches the nickel is crucial to prevent nitriding. As we have seen, this can be solved with internal catalyst layers, as demonstrated with iron by Pan et al. [93], amongst others. A recent study by Zheng et al. [100] concluded that amongst cheap ammonia decomposition catalysts Ni, Fe, Cu and 304 stainless steel, Ni performed best followed by Fe and 304, who performed almost equally, while Cu had the poorest performance. Removing or reducing the dependency on nickel to prevent nitriding is a topic under wide investigation, where alloying of Ni with other metals is more and more frequently tested to ensure stable and efficient ADR [15].

Molouk et al. [101] compared the much-used SOFC-O anodes Ni-YSZ and Ni-GDC and

found that the latter had a higher activity towards ammonia decomposition at 600 °C. The mixed ionic electronic conducting properties of GDC under reducing atmospheres were also stated to provide better performance. Conventional Ni-BCY and Ni-BZY PCFC anodes have shown higher activity towards ammonia decomposition than SOFC-O SDC and YSZ materials, with close to complete ammonia decomposition at 600 °C [102]. The basicity provided by the barium enhances the dehydrogenation rate and also shows better NH_3 adsorption and N_2 desorption [99, 103].

Hydrogen poisoning is a challenge at operating temperatures below 600°C, as hydrogen tends to be adsorbed to the catalytic reaction sites, hence, reducing the ammonia decomposition [104]. Yang et al. [72] studied the effect of hydrogen poisoning on ammonia decomposition, where a Ni-BCY25 ($BaCe_{0.75}Y_{0.25}O_{3-\delta}$) anode was compared with conventional SOFC-O Ni-GDC and Ni-YSZ anodes. Ni-BCY25 had superior resistance to hydrogen poisoning compared to conventional anodes. The poisoning effect, however, was relieved at higher temperatures for all materials, due to weaker adsorption of H_2. The steam content in the fuel mix and how this affected the ammonia conversion rate was also investigated. Here, Ni-BCY25 was inferior to the conventional anodes, as a decrease from 98% to 55% ammonia conversion could be seen with only a small addition of 0.8% steam in the fuel mix. The Ni-BCY25 was more susceptible to adsorbing water at the active sites, hence preventing ammonia decomposition.

Ammonia decomposition is mainly determined by temperature and catalyst materials, but as discussed above, factors such as water content in the fuel can have severe effects on some materials. Flow rates are also an important aspect that affects ammonia decomposition, hence performance. Lower flow rates will give the ammonia more time in contact with the catalysts, which increases conversion rates [16]. On the other hand, flow rates should be high enough to provide sufficient hydrogen production without flushing the produced hydrogen away. Ensuring optimal fuel utilisation and anode conditions should be done on a case-to-case basis, based on the materials and temperatures applied.

3.3.2 Nitric oxide production

As O^{2-} migrates through the electrolyte to the anode in SOFC-Os, the reaction between O_2 and N_2 from ammonia to produce NOx at the anode has been a recurring concern in

several papers [11, 13, 105]. The possibility of NOx production is absolutely present if we look back to Vayenas and Farr's first trials with the goal of producing nitric oxide in a SOFC with Pt electrodes. A percentage of 60% NO was seen in the exhaust when the conditions were tuned towards NO selectivity. These conditions included temperatures between 600-900 °C, and a low NH_3 molar flow rate, obtained through long residence time or low concentrations of ammonia in the fuel feed. In a system where the desired output is electricity and not NO, such low flow rates or low ammonia concentrations are not seen, hence, no studies with exhaust analyses in this review have reported observing any NOx [10, 60, 70, 80]. If, however, NOx is to be seen in the exhaust in larger-scale stacks, the technologies for reducing these emissions through selective catalytic or non-catalytic reduction of NOx are well developed [106, 107].

3.4 Anion exchange membrane fuel cells

Unlike SOFCs, which are foreseen in larger scale CHP powerplants and also maritime applications, AEMFCs provide an opportunity to use ammonia also for low-temperature and vehicular applications. PEMFCs are currently the most extensively used low-temperature fuel cell for most applications, and are, for example, used in H_2-fuelled cars today. Recently, however, ammonia was also successfully demonstrated to power a golf cart, through the indirect use in PEMFC [108]. The anion exchange membrane fuel cell can be regarded as the inverse technology of PEMFC, but can, unlike PEMFC, function in an ammonia atmosphere. The AEMFC stems from the traditional and much-used alkaline fuel cell, which relies on an aqueous KOH or NaOH electrolyte. Cairns et al. [109] was amongst the first to test ammonia in an alkaline fuel cell with conventional Pt electrodes in 1968. Here, ammonia was stated to be the best-performing fuel for these cells after hydrogen and hydrazine (N_2H_4). The development towards the use of alkaline polymer membranes in fuel cells was motivated by the wish to make a more compact cell that also could avoid electrolyte leakage, but still exploit the advantages of an alkaline environment. For example, the less corrosive alkaline environments allow for the use of non-noble catalysts as opposed to PEMFCs which are highly dependent on expensive platinum-based electrodes. Moreover, the alkaline atmosphere also allows for faster ORR kinetics [110]. Agel et al. [111] explored the possibility of using an alkaline polymer electrolyte in fuel cells in 2001.

Before this, alkaline polymer membranes had been used in batteries [112]. Promising results were achieved with a power density of 42 mW/cm^2 at 25°C, 1 atm and H_2/O_2 feed. Lan and Tao [113] were amongst the first to report the use of ammonia in AEMFCs in 2010, and since then a steady increase in performance has been seen, as materials have been tested and optimised.

3.4.1 Recent progress

Lan and Tao's experiments included testing of three fuel cell set-ups, two of whom are presented in Table 3.3. The first cell with a PtRu anode yielded very low PPDs of only 0.75 mW/cm^2, even when fed with pure O_2 as oxidant, compared to air for the other one, which achieved a PPD of around 9 mW/cm^2 with the same aqueous NH_3 solution. Moreover, the first cell did not reach the equilibrium OCV before half an hour had passed, which points to very slow kinetics. The second cell with Cr-decorated Ni, reached OCV equilibrium after 8 minutes. The increase in kinetics was ascribed to the much more active nano-sized nickel catalyst. Moreover, in the latter cell, aqueous ammonia performed better than both gaseous hydrogen and gaseous ammonia, which performed almost equally. The reason for this was suggested to be improved anode/electrolyte interface reactions, as the ionised $NH_3 - H_2O$ solution provided OH^- ions. This would lead to a mixed OH^-/e^- conduction at the anode, which could decrease polarisation.

Table 3.3: A selection of ammonia-fed AEMFCs and performances reported in the literature.

Anode/ cathode	Fuel composition	Temp. (°C)	Peak power density (mW/cm^2)	OCV	Reference/ year
PtRu-C/MnO_2-C	35 wt% aq NH_3-H_2O solution	room temp	0.75	~0.85	[114]/2010
Cr-decorated Ni-C/MnO_2-C	35 wt% aq NH_3-H_2O solution	room temp	~9	~0.8	[114]/2010
	Gaseous NH_3		~ 5	~0.72	
PtRh-C/Pt-C	3 M KOH, 3 M NH_4OH	50	5.37	0.68	[113]/2015
PtIr-C/Fe-N-C	16 M aq NH_3 solution	120	180	0.68	[115]/2020
PtRu-C/Pd-C	3 M NH_3 + 3 M KOH	95	20.7	0.67	[52]/2022
PtIr-C/ $MnCo_2O_4$**	7 M NH_3 + 3 M KOH	90	410		[116]/2022
$Ni_4Cu_5Fe_x$-C/ $Ni_4Cu_5Fe_x$-C	7 M NH_3H_2O + 3 M KOH	80	8.9	0.62	[36]/2022
PtIr-C/ $LaCr_{0.25}Fe_{0.25}Co_{0.}$	7 M NH_3H_2O + 1 M KOH	80	30.1	0.71	[117]/2023

**: 5 cell stack

In 2012, Suzuki et al. [54] tested three different anode catalysts with different fuel configurations; an alkaline aqueous ammonia solution, humidified and dry gaseous ammonia and humidified hydrogen gas were fed to the AEMFC at 50°C. For the humidified NH_3 and H_2 one could see a large drop in the OCV when switching from hydrogen to ammonia as seen in Figure 3.6. The figure also shows that Pt-Ru/C had the best AOR activity, while for wet hydrogen, the catalysts performed very similarly. The highest PPD attained with gaseous ammonia was reported to be 4.8 mW/cm^2. The study also reported the main explanation for the deactivation under humidified ammonia gas feed to be the adsorption of N_{ad} who poisoned the catalyst. Moreover, ammonia fuel crossover was shown to be dependent on wet conditions to occur.

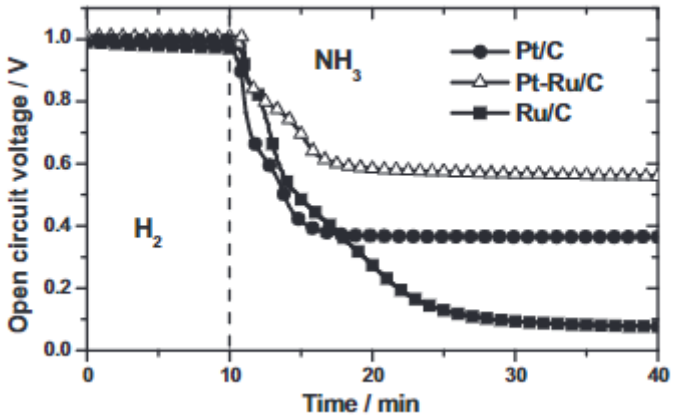

Figure 3.6: Operational voltage of an AEMFC at 50 °C tested with three different anodes. The dashed line indicates a switch of fuel from humidified H_2 gas to humidified NH_3 gas. Reprinted from Suzuki et al. [54], open access .

The viability of using gaseous ammonia in AEMFCs was also studied by Zhao et al. [118]. To improve the poor performance connected with gaseous ammonia fuel, operational parameters humidity and operating temperature were studied. First dry ammonia gas was introduced, resulting in a dried-out membrane and very high resistance, which clearly demonstrated the need for humidity to enable ionic conduction. Increasing the relative humidity by elevating the temperature was shown to rise both OCV and PPD. The explanation for the improvement was ascribed partly to increased AOR kinetics, partly to enhanced electrode ionic conduction, and to a much smaller degree, improved membrane ionic conduction.

Several papers have shown that having KOH in the fuel feed increases DA-AEMFC performance [52, 116, 119] and that higher concentrations of KOH will yield higher power densities up till a certain point [113]. The improvement is mainly attributed to a smaller charge transfer resistance [120]. Assumpcao et al. [113] found that a concentration of 3 M KOH and 3 M NH_4OH gave the best PPD in their cell. They also varied the concentration of NH_4OH between 1 and 5 M, but that did not affect the PPD significantly, indicating that the ammonia oxidation reaction is very slow in general. The authors argued that KOH had the role of increasing an otherwise insufficient anode/membrane transport, and called for further investigation into the interface processes in these fuel cells [113].

It should be discussed whether moving away from the traditional aqueous alkaline electrolyte is a feasible direction to take when aqueous KOH still has to be used with the ammonia fuel feed for the cell to perform. Efforts have, however, been made recently to remove the KOH from the fuel feed. Achrai et al. [115] wanted to create a KOH-free anode feed, and managed to generate a promising PPD of 180 mW/cm^2 at 120°C in their cell (see Table 3.3). Still, when tested with 12 M NH_3 and 2.5 M KOH, the PPD was higher (280 mW/cm^2 at 100°C). The reasoning behind a KOH-free anode feed was to increase the feasibility for practical applications like in vehicles. Since there is no consumption of KOH in the cell, an additional system to store and redistribute the base would demand more space, as opposed to the ammonia which is decomposed and consumed. An additional advantage of avoiding aqueous KOH was the reduced risk of corrosion.

Jeerh et al. first designed [110] and then optimised [117] an AEMFC with a non-noble perovskite oxide cathode $LaCr_{0.25}Fe_{0.25}Co_{0.5}O_{3-\delta}$ (LCFCO). The cathode configuration that contributed to the highest PPD is shown in Table 3.3. The cathode catalyst layer was optimised by varying the wt% of carbon black, Polytetrafluoroethylene (PTFE) and ionomer at the perovskite. The carbon was added to increase electrical conductivity, hence reducing ohmic resistance, and the hydrophobic PTFE was optimised to ensure sufficient transport of water away from the cathode side to prevent flooding of the electrolyte. A well-working ionomer network at the cathode is crucial for ionic transportation, enhancing the reaction sites at the catalyst interface. Physical compatibility between the ionomer and the membrane is a prerequisite. The optimal wt%s found were 50 wt% carbon, 10 wt% PTFE and 20 wt% ionomers, relative to the perovskite weight. The performance of

the LCFCO cathode was compared with a commercial Pt/C cathode in a similar system. The performances were almost equal, with 30.1 mW/cm^2 and 32 mW/cm^2, respectively, but the LCFCO had higher OCV with 0.71 V vs 0.6 V. Both cells experienced an increase in performance with increasing temperatures.

An important step towards the scale-up of DA-AEMs is Wang et al.'s [116] demonstrated 75 W stack, consisting of 5 AEMFCs, which were reported to achieve a PPD of 410 mW/cm^2. Also here PTFE was incorporated into the cathode catalyst layer to prevent cell flooding. It was shown that the chosen catalyst material $MnCo_2O_4$ was not affected substantially in contact with the ammonia crossing the membrane. A durability test was also executed for 80 hours at 100 °C and a current density of 300 mA/cm^2. A steady decrease could be seen in the cell voltage, and this drop was ascribed to the degradation of the membrane at these conditions (3 M KOH and near max temperature tolerance), which also caused increased ammonia crossover. The authors further suggested using the state-of-the-art developed stack prototype with liquid ammonia to power a drone. The proposed system can be seen in Figure 3.7A. Based on the stack measurements, a calculated system efficiency of 17% was expected if the ammonia crossover rate was a realistic 346 mA/cm^2 at voltage and current density conditions of 0.47 V and 300 mA/cm^2. If, however, the ammonia crossover could be reduced to less than 25 mA/cm^2, a system efficiency of ∼35% could be expected (Fig. 3.7B). Higher operational temperatures or better membranes were also solutions for potential improvements. Figure 3.7C shows the energy densities of the potential system compared to a lithium-ion battery system and a PEMFC system, which shows that at current performances, PEMFC would be the best choice when considering gravimetric energy density. However, the target AEMFC system shows superior energy densities, both gravimetric and volumetric, which yields promising future potential applications.

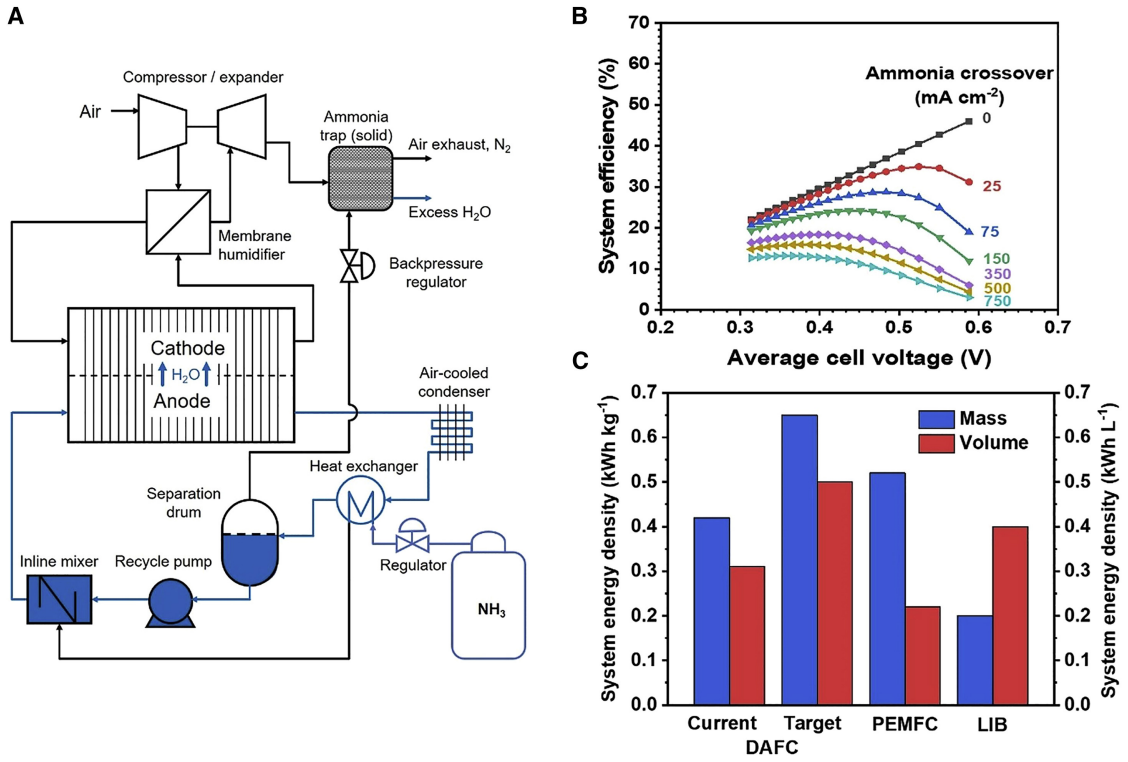

Figure 3.7: A) Schematic of an AEMFC drone powering system. B) Theoretic system efficiency based on different ammonia crossover rates. C) A comparison of the volumetric and gravimetric system energy density between a drone powered by a lithium-ion battery (LIB), PEMFC and AEMFC (here called DAFC) with current and target performances. Reprinted from Wang et al. [116], open access.

3.4.2 Challenges

As Table 3.3 shows, the actual OCVs are, in general, much lower than the theoretical 1.17 V. The greatest hindrance for DA-AEMFCs is the slow ammonia oxidation reaction and the inadequacy of AOR catalysts. Further, ammonia crossover and insufficient membrane/electrode charge transfer are lowering the overall performance. A short lifetime of the membrane itself is also a general problem for AEMFCs, caused by the decomposition of the QA functional groups under strongly alkaline conditions [121].

AOR proceeds via a number of dehydrogenation steps as shown in Table 2.3, and many catalysts are prone to adsorb these intermediate compounds, which causes a poisoning effect [119]. Efforts have been made to explore catalysts to increase the kinetics of the slow AOR. Within the noble catalysts, systematic research has revealed that the PtIr alloy provides the highest AOR activity and also the lowest ammonia oxidation potential [36]. Amongst the non-noble materials, Ni, as previously seen, together with Fe, Cu and Co is recognised as the most promising material [36], but as seen from the reviewed

papers in the previous section, the transition away from noble anode catalysts is still rather slow. Finding a catalyst, preferably non-noble, that balances the properties of weak N_{ad} adsorption and stronger N_2 recombination, while at the same time optimising anode structure and operating conditions towards effective AOR is an important and ongoing research topic [14].

Ammonia crossover increases both at higher anode pressures and higher fuel flow rates and at higher humidity for gaseous NH_3-feed [52, 122]. The problem with ammonia crossover is first and foremost connected to the loss of reactants, and not so much to the poisoning of the cathode catalyst [116]. However, dilution at the cathode side will most likely have a negative effect on the already sluggish ORR kinetics. The highest amount of ammonia crossover is seen with aqueous ammonia. Additionally, aqueous ammonia has several other disadvantages, such as the elevated risk of cathode flooding and the increase in complexity of the system connected to aqueous solutions. If ammonia is stored anhydrous, the combination of unreacted aqueous fuel with anhydrous ammonia complicates matters, and if the fuel is stored in an aqueous form, energy density is lowered [118].

While humidified H_2 gas in AEMFCs have shown OCVs of 1 V and negligible fuel crossover, ammonia has a way to go. An example of hydrogen crossover numbers in AEM is 0.41 mA/cm^2 with wet H_2 (100% relative humidity) at 50°C [123]. Also here crossover was increased at higher relative humidity, but still, the target crossover rate of 25 mA/cm^2 by Wang et al. [116] is still 100 orders of magnitude larger in comparison.

Currently, the OH^- conducting membrane is both less durable and less conductive than the PEM, as H^+ transport is more facile. Another problem is the insufficient development of ionomers to ensure sufficient OH^--transport at the electrode/electrolyte interface [124]. For PEMs, ionomers are well commercialised, but efforts need to be made to develop stable and highly conductive ionomers for AEMFCs. However, AEMFCs in general, and especially ammonia-fed AEMFCs are very new technology, and the impressive performance improvements achieved in such a short time should not be undermined. Even if it is still a way ahead for the AEMFC to compete with the well-established PEMFC, the beginning-of-life accomplishments make out promising low-temperature direct ammonia fuel cell technology.

CHAPTER 4

Conclusion and future perspectives

The working of and recent research within direct ammonia fuel cells (solid oxide and anion exchange membrane technology) has been investigated. Ammonia as a fuel for fuel cells stands out as a promising alternative to conventional hydrocarbon and hydrogen fuels due to its carbon-free nature, and much higher volumetric energy density, respectively. Moreover, the direct ammonia feed to the fuel cells instead of pre-cracking can reduce cost and spatial needs.

High-performing fuel cells have been developed within both oxide ion and proton-conducting SOFC, where nickel enables both ammonia decomposition and hydrogen oxidation. Recent achievements include high PPDs of ~ 1600 mW/cm^2 for a Fe-decorated Ni-BZCYYb|BZCYYb|PBSCF PCFC, and ~ 1890 mW/cm^2 for a $CeO_{2-\delta}$ infiltrated Ni-YSZ|YSZ|PBCC SOFC-O, which is around 80% of the performances of H_2 in the same cells. When assessing the commercial-scale viability of these technologies, performance and stability is equally important. High temperatures are beneficial both for improving ADR kinetics, which is the key to high performance, and preventing nickel nitriding from deteriorating the anode structure. Moreover, many popular anode materials are prone to hydrogen- and steam poisoning at temperatures below 600°C. However, as trends are moving towards lower operational temperatures to reduce start-up time and mechanical degradation, more research towards effective and durable low-temperature catalysts for ammonia decomposition is crucial to enable commercialisation.

The ammonia-fed anion exchange membrane fuel cell is a technology in its infancy but extensive research has resulted in an impressive increase in performance in the last decade,

reaching PPDs above 400 mW/cm^2 in a 5-cell stack. However, degradation is an issue also here, mostly connected to the membrane itself. For AEMFCs, slow ammonia oxidation kinetics and poor surface charge transfer are the main mechanisms hindering performance. Also, fuel crossover is a significant issue compared to when fuelled with hydrogen. Until now, mostly noble Pt-based materials have been used as ammonia oxidation catalysts, even if the alkaline environment allows for the use of non-noble materials. Economical factors should be taken into consideration when evaluating commercial viability. PEMFCs have been commercialised regardless of the dependence on Pt-based catalysts, but for AEMFCs to stand up as an alternative, the key enabler is the possibility of using non-noble materials as well as a higher degree of fuel flexibility.

A key research topic towards scale-up for ammonia-fed AEMFCs is managing to get rid of the dependence on KOH in the fuel mix, ensuring sufficient ammonia oxidation and charge transfer with water and ammonia alone. Further membrane development and a proper understanding of the charge transfer and oxidation processes are necessary to overcome these challenges.

Despite the challenges, promising results are found for all technologies. DA-SOFC-O has proved viability at a larger scale and a 2 MW stack is currently being developed for ship propulsion in the ShipFC project. Having proven performances close to H_2 in commercial cells, the remaining step is further improved durability. PCFC technology continues stepping forward, closing the gap to SOFC-O with its sought-after ability to operate at lower temperatures. The important findings on the role of Fe to protect nickel from nitriding as well as ensuring excellent ammonia decomposition have yielded comparable PPDs to SOFC-O. The anion exchange membrane stands out as a very promising low-temperature ammonia technology but encounters several challenges to be solved before it can compete with the well-established PEM fuel cell. Together, the diverse and numerous research efforts make out solid advocacy for the continuation of ammonia fuel cell development, as a promising carbon-free technology.

Bibliography

[1] IEA (2022), World Energy Outlook 2022, IEA, Paris. https://www.iea.org/reports/world-energy-outlook-2022, License: CC BY 4.0 (report); CC BY NC SA 4.0 (Annex A).

[2] DNV (2022), Energy transition outlook.

[3] Ibrahim Dincer and Osamah Siddiqui. *Ammonia Fuel Cells*. Elsevier, 2020.

[4] National Aeronautics Kenneth A. Burke and Space Administration (NASA). Fuel Cells For Space Science Applications, 2003.

[5] DNV (2022), Hydrogen forecast to 2050.

[6] Coradia ilint regional train. https://www.railway-technology.com/projects/coradia-ilint-regional-train/, accessed 03.02.23.

[7] Kevin HR Rouwenhorst and Gabriel Castellanos. Innovation outlook: Renewable ammonia. IRENA, 2022.

[8] Muhammad Aziz, Agung Tri Wijayanta, and Asep Bayu Dani Nandiyanto. Ammonia as Effective Hydrogen Storage: A Review on Production, Storage and Utilization. *Energies*, 13(12):3062, 6 2020.

[9] Osamah Siddiqui and Ibrahim Dincer. A review and comparative assessment of direct ammonia fuel cells. *Thermal Science and Engineering Progress*, 5:568–578, 3 2018.

[10] M. Kishimoto, H. Muroyama, S. Suzuki, M. Saito, T. Koide, Y. Takahashi, T. Horiuchi, H. Yamasaki, S. Matsumoto, H. Kubo, N. Takahashi, A. Okabe, S. Ueguchi, M. Jun, A. Tateno, T. Matsuo, T. Matsui, H. Iwai, H. Yoshida, and K. Eguchi. Development of 1 kW-class Ammonia-fueled Solid Oxide Fuel Cell Stack. *Fuel Cells*, 20(1):80–88, 2 2020.

[11] Georgina Jeerh, Mengfei Zhang, and Shanwen Tao. Recent progress in ammonia fuel cells and their potential applications, 1 2021.

[12] Shambhu Singh Rathore, Saheli Biswas, Daniel Fini, Aniruddha P. Kulkarni, and Sarbjit Giddey. Direct ammonia solid-oxide fuel cells: A review of progress and prospects. *International Journal of Hydrogen Energy*, 46(71):35365–35384, 10 2021.

[13] Muskan Sonker, Saurabh Kr Tiwary, Nehil Shreyash, Sushant Bajpai, Mainak Ray, Sanjay Kumar Kar, and M. S. Balathanigaimani. Ammonia as an alternative fuel for vehicular applications: Paving the way for adsorbed ammonia and direct ammonia fuel cells. *Journal of Cleaner Production*, 376:133960, 11 2022.

[14] Yuqi Guo, Zhefei Pan, and Liang An. Carbon-free sustainable energy technology: Direct ammonia fuel cells. *Journal of Power Sources*, 476:228454, 11 2020.

[15] Bin Wang, Tao Li, Feng Gong, Mohd Hafiz Dzarfan Othman, and Rui Xiao. Ammonia as a green energy carrier: Electrochemical synthesis and direct ammonia fuel cell - a comprehensive review. *Fuel Processing Technology*, 235:107380, 10 2022.

[16] Qidong Xu, Zengjia Guo, Lingchao Xia, Qijiao He, Zheng Li, Idris Temitope Bello, Keqing Zheng, and Meng Ni. A comprehensive review of solid oxide fuel cells operating on various promising alternative fuels, 2 2022.

[17] Zhijian Wan, Youkun Tao, Jing Shao, Yinghui Zhang, and Hengzhi You. Ammonia as an effective hydrogen carrier and a clean fuel for solid oxide fuel cells. *Energy Conversion and Management*, 228:113729, 1 2021.

[18] Shimshon Gottesfeld. The Direct Ammonia Fuel Cell and a Common Pattern of Electrocatalytic Processes. *Journal of The Electrochemical Society*, 165(15):J3405–J3412, 2018.

[19] IEA (2021), Ammonia Technology Roadmap, IEA, Paris . `https://www.iea.org/reports/ammonia-technology-roadmap`, License: CC BY 4.0.

[20] João Sousa Cardoso, Valter Silva, Rodolfo C. Rocha, Matthew J. Hall, Mário Costa, and Daniela Eusébio. Ammonia as an energy vector: Current and future prospects for low-carbon fuel applications in internal combustion engines. *Journal of Cleaner Production*, 296:126562, 5 2021.

[21] Cinzia Tornatore, Luca Marchitto, Pino Sabia, and Mara De Joannon. Ammonia as Green Fuel in Internal Combustion Engines: State-of-the-Art and Future Perspectives, 7 2022.

[22] POWER Magazine. Mitsubishi Power Developing 100% Ammonia-Capable Gas Turbine. `https://www.powermag.com/mitsubishi-power-developing-100-ammonia-capable-gas-turbine/`, accessed 09.02.23.

[23] Vasileios Kyriakou, Ioannis Garagounis, Anastasios Vourros, Eirini Vasileiou, and Michael Stoukides. An Electrochemical Haber-Bosch Process. *Joule*, 4(1):142–158, 1 2020.

[24] Merics.org. What is green hydrogen and how is it made? `https://merics.org/en/report/chinas-nascent-green-hydrogen-sector-how-policy-research-and-business-are-forging-new`, accessed 09.02.23.

[25] A. Ajanovic, M. Sayer, and R. Haas. The economics and the environmental benignity of different colors of hydrogen. *International Journal of Hydrogen Energy*, 47(57):24136–24154, 7 2022.

[26] Kevin Dillman and Jukka Heinonen. Towards a Safe Hydrogen Economy: An Absolute Climate Sustainability Assessment of Hydrogen Production. *Climate*, 11(1):25, 1 2023.

[27] Daniel Addokwei Tetteh and Saeed Salehi. The Blue Hydrogen Economy: A Promising Option for the Near-to-Mid-Term Energy Transition. *Journal of Energy Resources Technology*, 145(4), 4 2023.

[28] Changjie Li, Ye Liu, Bing Xu, and Zheshu Ma. Finite Time Thermodynamic Optimization of an Irreversible Proton Exchange Membrane Fuel Cell for Vehicle Use. *Processes*, 7(7):419, 7 2019.

[29] Andrew L Dicks and David AJ Rand. *Fuel cell systems explained*. John Wiley &

Sons, 2018.

[30] Jarosław Milewski and J Lewandowski. Analysis of design and construction of solid oxide fuel cell in terms of their dynamic operation. *Archivum Combustionis*, 30(3):145–154, 2010.

[31] Michele Zendrini, Matteo Testi, Martina Trini, Penchini Daniele, Jan Van Herle, and Luigi Crema. Assessment of ammonia as energy carrier in the use with reversible solid oxide cells. *International Journal of Hydrogen Energy*, 46(58):30112–30123, 8 2021.

[32] Simon Ristig, Michael Poschmann, Jan Folke, Oscar Gómez-Cápiro, Zongkun Chen, Nuria Sanchez-Bastardo, Robert Schlögl, Saskia Heumann, and Holger Ruland. Ammonia Decomposition in the Process Chain for a Renewable Hydrogen Supply. *Chemie Ingenieur Technik*, 94(10):1413–1425, 10 2022.

[33] Atsushi Takahashi and Tadahiro Fujitani. Kinetic Analysis of Decomposition of Ammonia over Nickel and Ruthenium Catalysts. *Journal of Chemical Engineering of Japan*, 49(1):22–28, 2016.

[34] NP Brandon and DJ Brett. Engineering porous materials for fuel cell applications. *Philosophical Transactions of the Royal Society A: Mathematical, Physical and Engineering Sciences*, 364(1838):147–159, 2006.

[35] Sossina M. Haile. Materials for fuel cells. *Materials Today*, 6(3):24–29, 3 2003.

[36] Mengfei Zhang, Jie Zhang, Georgina Jeerh, Peimiao Zou, Boyao Sun, Marc Walker, Kui Xie, and Shanwen Tao. A symmetric direct ammonia fuel cell using ternary NiCuFe alloy embedded in a carbon network as electrodes. *Journal of Materials Chemistry A*, 10(36):18701–18713, 2022.

[37] Truls Norby. Mena 1001; materialer, energi og nanoteknologi - kap. 3, termodynamikk. University Lecture, 2017.

[38] Allen J Bard, Larry R Faulkner, and Henry S White. *Electrochemical methods: fundamentals and applications*. John Wiley & Sons, 2022.

[39] LibreTexts chemistry. Activities and their effects on equilibria. `https://chem.libretexts.org/Bookshelves/Physical_and_Theoretical_Chemistry_Textbook_Maps/Supplemental_Modules_(Physical_and_Theoretical_Chemistry)/Physical_Properties_of_Matter/Solutions_and_Mixtures/Nonideal_Solutions/Activities_and_their_Effects_on_Equilibria`, accessed 06.03.23.

[40] Truls Norby. Personal communication.

[41] Antoine-Amaury Guillerm. Assessment of a solid oxide fuel cell powering a full electric aircraft subsystem architecture, 2020.

[42] M. Schoemaker, U. Misz, P. Beckhaus, and A. Heinzel. Evaluation of Hydrogen Crossover through Fuel Cell Membranes. *Fuel Cells*, 14(3):412–415, 6 2014.

[43] Juan F. Basbus, Mauricio D. Arce, Federico R. Napolitano, Horacio E. Troiani, José A. Alonso, Martín E. Saleta, Miguel A. González, Gabriel J. Cuello, María T. Fernández-Díaz, Miguel Pardo Sainz, Nikolaos Bonanos, Catalina E. Jimenez, Lars Giebeler, Santiago J.A. Figueroa, Alberto Caneiro, Adriana C. Serquis, and Lil-

iana V. Mogni. Revisiting the Crystal Structure of BaCe0.4Zr0.4Y0.2O3-δ Proton Conducting Perovskite and Its Correlation with Transport Properties. *ACS Applied Energy Materials*, 3(3):2881–2892, 3 2020.

[44] S. Rauf, B. Zhu, M.A.K.Y. Shah, Z. Tayyab, S. Attique, N. Ali, N. Mushtaq, M.I. Asghar, P.D. Lund, and C.P. Yang. Low-temperature solid oxide fuel cells based on Tm-doped SrCeO2-δ semiconductor electrolytes. *Materials Today Energy*, 20:100661, 6 2021.

[45] N Bonanos, K Knigth, and B Ellis. Perovskite solid electrolytes: Structure, transport properties and fuel cell applications. *Solid State Ionics*, 79:161–170, 7 1995.

[46] Kamil M. Nowicki, George Carins, John Bayne, Chayopas Tupberg, Gavin J. Irvine, and John T. S. Irvine. Characterisation of direct ammonia proton conducting tubular ceramic fuel cells for maritime applications. *Journal of Materials Chemistry A*, 11(1):352–363, 2023.

[47] Jiafeng Cao, Chao Su, Yuexia Ji, Guangming Yang, and Zongping Shao. Recent advances and perspectives of fluorite and perovskite-based dual-ion conducting solid oxide fuel cells. *Journal of Energy Chemistry*, 57:406–427, 6 2021.

[48] Qiying Jiang, Sedigheh Faraji, David A. Slade, and Susan M. Stagg-Williams. A Review of Mixed Ionic and Electronic Conducting Ceramic Membranes as Oxygen Sources for High-Temperature Reactors. pages 235–273. 2011.

[49] Idoia Ruiz de Larramendi, Nagore Ortiz-Vitoriano, Isaen B. Dzul-Bautista, and Teófilo Rojo. Designing Perovskite Oxides for Solid Oxide Fuel Cells. In *Perovskite Materials - Synthesis, Characterisation, Properties, and Applications*. InTech, 2 2016.

[50] X.W. Dong, J.B. Zhuang, N.B. Huang, C.H. Liang, L.S. Xu, W. Li, S.C. Zhang, and M. Sun. Development of anion-exchange membrane for anion-exchange membrane fuel cells. *Materials Research Innovations*, 19(sup6):6–38, 6 2015.

[51] Takashi Hibino and Kazuyo Kobayashi. An intermediate-temperature alkaline fuel cell using an Sn 0.92 Sb 0.08 P 2 O 7-based hydroxide-ion-conducting electrolyte and electrodes. *Journal of Materials Chemistry A*, 1(4):1134–1140, 2013.

[52] Yun Liu, Zhefei Pan, Oladapo Christopher Esan, Xinhai Xu, and Liang An. Performance Characteristics of a Direct Ammonia Fuel Cell with an Anion Exchange Membrane. *Energy & Fuels*, 36(21):13203–13211, 11 2022.

[53] Dirk Henkensmeier, Malikah Najibah, Corinna Harms, Jan Žitka, Jaromír Hnát, and Karel Bouzek. Overview: State-of-the Art Commercial Membranes for Anion Exchange Membrane Water Electrolysis. *Journal of Electrochemical Energy Conversion and Storage*, 18(2), 5 2021.

[54] Shohei Suzuki, Hiroki Muroyama, Toshiaki Matsui, and Koichi Eguchi. Fundamental studies on direct ammonia fuel cell employing anion exchange membrane. *Journal of Power Sources*, 208:257–262, 6 2012.

[55] CG Vayenas and RD Farr. Cogeneration of electric energy and nitric oxide. *Science*, 208(4444):593–594, 1980.

[56] Roger D Farr and Costas G Vayenas. Ammonia high temperature solid electrolyte fuel cell. *Journal of The Electrochemical Society*, 127(7):1478, 1980.

[57] Adam Wojcik, Hugh Middleton, Ioannis Damopoulos, and Jan Van herle. Ammonia as a fuel in solid oxide fuel cells. *Journal of Power Sources*, 118(1-2):342–348, 5 2003.

[58] Qianli Ma, Jianjun Ma, Sa Zhou, Ruiqiang Yan, Jianfeng Gao, and Guangyao Meng. A high-performance ammonia-fueled SOFC based on a YSZ thin-film electrolyte. *Journal of Power Sources*, 164(1):86–89, 1 2007.

[59] Limin Liu, Kening Sun, Xiaoyan Wu, Xiaokun Li, Ming Zhang, Naiqing Zhang, and Xiaoliang Zhou. Improved performance of ammonia-fueled solid oxide fuel cell with SSZ thin film electrolyte and Ni-SSZ anode functional layer. *International Journal of Hydrogen Energy*, 37(14):10857–10865, 7 2012.

[60] Guangyao Meng, Cairong Jiang, Jianjun Ma, Qianli Ma, and Xingqin Liu. Comparative study on the performance of a SDC-based SOFC fueled by ammonia and hydrogen. *Journal of Power Sources*, 173(1):189–193, 11 2007.

[61] Kang Xu, Feng Zhu, Mingyang Hou, Canan Li, Hua Zhang, and Yu Chen. Activating and stabilizing the surface of anode for high-performing direct-ammonia solid oxide fuel cells. *Nano Research*, 16(2):2454–2462, 2 2023.

[62] Jiaqi Qian, Xiaoliang Zhou, Limin Liu, Jing Liu, Luomeng Zhao, Hanwen Shen, Xingguo Hu, Xinyuan Qian, Hanyu Chen, Xin Zhou, and Zhaohuan Wei. Direct ammonia low-temperature symmetrical solid oxide fuel cells with composite semiconductor electrolyte. *Electrochemistry Communications*, 135:107216, 2 2022.

[63] Xingtong Mao, Junkang Sang, Chengqiao Xi, Zhixiang Liu, Jun Yang, Wanbing Guan, Jianxin Wang, Changrong Xia, and Subhash C. Singhal. Performance evaluation of ammonia-fueled flat-tube solid oxide fuel cells with different build-in catalysts. *International Journal of Hydrogen Energy*, 47(55):23324–23334, 6 2022.

[64] Seongkook Oh, Min Jun Oh, Jongsup Hong, Kyung Joong Yoon, Ho-Il Ji, Jong-Ho Lee, Hyungmook Kang, Ji-Won Son, and Sungeun Yang. A comprehensive investigation of direct ammonia-fueled thin-film solid-oxide fuel cells: Performance, limitation, and prospects. *iScience*, 25(9):105009, 9 2022.

[65] Seongkook Oh, Joonsuk Park, Jeong Woo Shin, Byung Chan Yang, Jiaming Zhang, Dong Young Jang, and Jihwan An. High performance low-temperature solid oxide fuel cells with atomic layer deposited-yttria stabilized zirconia embedded thin film electrolyte. *Journal of Materials Chemistry A*, 6(17):7401–7408, 2018.

[66] Wei Zhang, Yixiao Cai, Baoyuan Wang, Hui Deng, Chu Feng, Wenjing Dong, Junjiao Li, and Bin Zhu. The fuel cells studies from ionic electrolyte Ce0.8Sm0.05Ca0.15O2-δ to the mixture layers with semiconductor Ni0.8Co0.15Al0.05LiO2-δ. *International Journal of Hydrogen Energy*, 41(41):18761–18768, 11 2016.

[67] Sea-Fue Wang, Yi-Le Liao, Yung-Fu Hsu, and Piotr Jasinski. Effects of Ni-NCAL and Ni–Ag electrodes on the cell performances of low-temperature solid oxide fuel cells with Sm0.2Ce0 · 8O2-δ electrolyte at various temperatures. *International Journal of Hydrogen Energy*, 47(94):40067–40082, 12 2022.

[68] Michael M. Whiston, Inês M.L. Azevedo, Shawn Litster, Constantine Samaras, Kate S. Whitefoot, and Jay F. Whitacre. Meeting U.S. Solid Oxide Fuel Cell Targets. *Joule*, 3(9):2060–2065, 9 2019.

[69] Liangzhu Zhu, Chris Cadigan, Chuancheng Duan, Jake Huang, Liuzhen Bian, Long

Le, Carolina H. Hernandez, Victoria Avance, Ryan O'Hayre, and Neal P. Sullivan. Ammonia-fed reversible protonic ceramic fuel cells with Ru-based catalyst. *Communications Chemistry*, 4(1):121, 8 2021.

[70] Anke Hagen, Hendrik Langnickel, and Xiufu Sun. Operation of solid oxide fuel cells with alternative hydrogen carriers. *International Journal of Hydrogen Energy*, 44(33):18382–18392, 7 2019.

[71] Sanaz Zarabi Golkhatmi, Muhammad Imran Asghar, and Peter D. Lund. A review on solid oxide fuel cell durability: Latest progress, mechanisms, and study tools. *Renewable and Sustainable Energy Reviews*, 161:112339, 6 2022.

[72] Jun Yang, Ahmed Fathi Salem Molouk, Takeou Okanishi, Hiroki Muroyama, Toshiaki Matsui, and Koichi Eguchi. Electrochemical and catalytic properties of Ni/BaCe0. 75Y0. 25O3- δ anode for direct ammonia-fueled solid oxide fuel cells. *ACS applied materials & interfaces*, 7(13):7406–7412, 2015.

[73] Jun Yang, Ahmed Fathi Salem Molouk, Takeou Okanishi, Hiroki Muroyama, Toshiaki Matsui, and Koichi Eguchi. A Stability Study of Ni/Yttria-Stabilized Zirconia Anode for Direct Ammonia Solid Oxide Fuel Cells. *ACS Applied Materials & Interfaces*, 7(51):28701–28707, 12 2015.

[74] Skipsrevyen. Alma Clean Power har nådd en viktig milepæl: – Glade for at vårt design har blitt godkjent. `https://www.skipsrevyen.no/alma-clean-power-dnv-sofc/alma-clean-power-har-nadd-en-viktig-milepael-glade-for-at-vart-design-har-blitt-godkjent/1481003`, accessed 19.04.23.

[75] Phan Anh Duong, Borim Ryu, Chongmin Kim, Jinuk Lee, and Hokeun Kang. Energy and Exergy Analysis of an Ammonia Fuel Cell Integrated System for Marine Vessels. *Energies*, 15(9):3331, 5 2022.

[76] M.F. Ezzat and I. Dincer. Energy and exergy analyses of a novel ammonia combined power plant operating with gas turbine and solid oxide fuel cell systems. *Energy*, 194:116750, 3 2020.

[77] Thai-Quyen Quach, Van-Tien Giap, Dong Keun Lee, Torres Pineda Israel, and Kook Young Ahn. High-efficiency ammonia-fed solid oxide fuel cell systems for distributed power generation. *Applied Energy*, 324:119718, 10 2022.

[78] G. Cinti, G. Discepoli, E. Sisani, and U. Desideri. SOFC operating with ammonia: Stack test and system analysis. *International Journal of Hydrogen Energy*, 41(31):13583–13590, 8 2016.

[79] T. Okanishi, K. Okura, A. Srifa, H. Muroyama, T. Matsui, M. Kishimoto, M. Saito, H. Iwai, H. Yoshida, M. Saito, T. Koide, H. Iwai, S. Suzuki, Y. Takahashi, T. Horiuchi, H. Yamasaki, S. Matsumoto, S. Yumoto, H. Kubo, J. Kawahara, A. Okabe, Y. Kikkawa, T. Isomura, and K. Eguchi. Comparative Study of Ammonia-fueled Solid Oxide Fuel Cell Systems. *Fuel Cells*, 17(3):383–390, 6 2017.

[80] Bernhard Stoeckl, Michael Preininger, Vanja Subotić, Stefan Megel, Christoph Folgner, and Christoph Hochenauer. Towards a wastewater energy recovery system: The utilization of humidified ammonia by a solid oxide fuel cell stack. *Journal of Power Sources*, 450:227608, 2 2020.

[81] ShipFC. `https://shipfc.eu/`, accessed 19.04.23.

[82] J. Kim, S. Sengodan, S. Kim, O. Kwon, Y. Bu, and G. Kim. Proton conducting

oxides: A review of materials and applications for renewable energy conversion and storage. *Renewable and Sustainable Energy Reviews*, 109:606–618, 7 2019.

[83] H. Iwahara, T. Esaka, H. Uchida, and N. Maeda. Proton conduction in sintered oxides and its application to steam electrolysis for hydrogen production. *Solid State Ionics*, 3-4:359–363, 1981.

[84] Arpan Kumar Nayak and Ananta Sasmal. Recent advance on fundamental properties and synthesis of barium zirconate for proton conducting ceramic fuel cell. *Journal of Cleaner Production*, 386:135827, 2 2023.

[85] Dan Cao, Mingyang Zhou, Xiaomin Yan, Zhijun Liu, and Jiang Liu. High performance low-temperature tubular protonic ceramic fuel cells based on barium cerate-zirconate electrolyte. *Electrochemistry Communications*, 125:106986, 4 2021.

[86] Jiafeng Cao, Yuexia Ji, and Zongping Shao. Perovskites for protonic ceramic fuel cells: a review. *Energy & Environmental Science*, 15(6):2200–2232, 2022.

[87] Idris Temitope Bello, Shuo Zhai, Qijiao He, Chun Cheng, Yawen Dai, Bin Chen, Yuan Zhang, and Meng Ni. Materials development and prospective for protonic ceramic fuel cells. *International Journal of Energy Research*, 46(3):2212–2240, 3 2022.

[88] Yoshitaka Aoki, Tomoyuki Yamaguchi, Shohei Kobayashi, Damian Kowalski, Chunyu Zhu, and Hiroki Habazaki. High-efficiency direct ammonia fuel cells based on BaZr0. 1Ce0. 7Y0. 2O3- δ/Pd oxide-metal junctions. *Global Challenges*, 2(1):1700088, 2018.

[89] Heon Jun Jeong, Wanhyuk Chang, Beum Geun Seo, Yun Sung Choi, Keun Hee Kim, Dong Hwan Kim, and Joon Hyung Shim. High-Performance Ammonia Protonic Ceramic Fuel Cells Using a Pd Inter-Catalyst. *Small*, page 2208149, 3 2023.

[90] Limin Zhang and Weishen Yang. Direct ammonia solid oxide fuel cell based on thin proton-conducting electrolyte. *Journal of Power Sources*, 179(1):92–95, 4 2008.

[91] Fan He, Qinning Gao, Zuoqing Liu, Meiting Yang, Ran Ran, Guangming Yang, Wei Wang, Wei Zhou, and Zongping Shao. A New Pd Doped Proton Conducting Perovskite Oxide with Multiple Functionalities for Efficient and Stable Power Generation from Ammonia at Reduced Temperatures. *Advanced Energy Materials*, 11(19):2003916, 5 2021.

[92] Hua Zhang, Yucun Zhou, Kai Pei, Yuxin Pan, Kang Xu, Yong Ding, Bote Zhao, Kotaro Sasaki, Yongman Choi, Yu Chen, and Meilin Liu. An efficient and durable anode for ammonia protonic ceramic fuel cells. *Energy and Environmental Science*, 15(1):287–295, 1 2022.

[93] Yuxin Pan, Hua Zhang, Kang Xu, Yucun Zhou, Bote Zhao, Wei Yuan, Kotaro Sasaki, YongMan Choi, Yu Chen, and Meilin Liu. A high-performance and durable direct NH3 tubular protonic ceramic fuel cell integrated with an internal catalyst layer. *Applied Catalysis B: Environmental*, 306:121071, 6 2022.

[94] Mingyang Hou, Yuxin Pan, and Yu Chen. Enhanced electrochemical activity and durability of a direct ammonia protonic ceramic fuel cell enabled by an internal catalyst layer. *Separation and Purification Technology*, 297:121483, 9 2022.

[95] H. Iwahara, H. Uchida, K. Ono, and K. Ogaki. Proton Conduction in Sintered Oxides Based on BaCeO3. *Journal of The Electrochemical Society*, 135(2):529–533,

2 1988.

[96] Robert J. Braun, Alexis Dubois, Kyle Ferguson, Chuancheng Duan, Canan Karakaya, Robert J. Kee, Huayang Zhu, Neal P Sullivan, Eric Tang, Michael Pastula, Anthony Wood, Tahir Joia, and Ryan O'Hayre. Development of kW-Scale Protonic Ceramic Fuel Cells and Systems. *ECS Transactions*, 91(1):997–1008, 7 2019.

[97] Xiandong Xiong, Jian Yu, Xiaojian Huang, Dan Zou, Yufei Song, Meigui Xu, Ran Ran, Wei Wang, Wei Zhou, and Zongping Shao. Slightly ruthenium doping enables better alloy nanoparticle exsolution of perovskite anode for high-performance direct-ammonia solid oxide fuel cells. *Journal of Materials Science & Technology*, 125:51–58, 10 2022.

[98] Yinghua Niu, Yucun Zhou, Weiqiang Lv, Yu Chen, Yanxiang Zhang, Weilin Zhang, Zheyu Luo, Nicholas Kane, Yong Ding, Luke Soule, Yuchen Liu, Weidong He, and Meilin Liu. Enhancing Oxygen Reduction Activity and Cr Tolerance of Solid Oxide Fuel Cell Cathodes by a Multiphase Catalyst Coating. *Advanced Functional Materials*, 31(19):2100034, 5 2021.

[99] Ainaa Nadhirah Zainon, Mahendra Rao Somalu, Audi Majdan Kamarul Bahrain, Andanastuti Muchtar, Nurul Akidah Baharuddin, Muhammed Ali S.A, Nafisah Osman, Abdullah Abdul Samat, Abul Kalam Azad, and Nigel P. Brandon. Challenges in using perovskite-based anode materials for solid oxide fuel cells with various fuels: a review. *International Journal of Hydrogen Energy*, 3 2023.

[100] Keqing Zheng, Yangtian Yan, Ya Sun, Jun Yang, Meng Zhu, Meng Ni, and Li Li. An experimental study of ammonia decomposition rates over cheap metal catalysts for solid oxide fuel cell anode. *International Journal of Hydrogen Energy*, 2 2023.

[101] Ahmed Fathi Salem Molouk, Jun Yang, Takeou Okanishi, Hiroki Muroyama, Toshiaki Matsui, and Koichi Eguchi. Comparative study on ammonia oxidation over Ni-based cermet anodes for solid oxide fuel cells. *Journal of Power Sources*, 305:72–79, 2 2016.

[102] Kazunari Miyazaki, Takeou Okanishi, Hiroki Muroyama, Toshiaki Matsui, and Koichi Eguchi. Development of Ni–Ba(Zr,Y)O3 cermet anodes for direct ammonia-fueled solid oxide fuel cells. *Journal of Power Sources*, 365:148–154, 10 2017.

[103] Ilaria Lucentini, Xènia Garcia, Xavier Vendrell, and Jordi Llorca. Review of the Decomposition of Ammonia to Generate Hydrogen. *Industrial & Engineering Chemistry Research*, 60(51):18560–18611, 12 2021.

[104] Kazunari Miyazaki, Hiroki Muroyama, Toshiaki Matsui, and Koichi Eguchi. Impact of the ammonia decomposition reaction over an anode on direct ammonia-fueled protonic ceramic fuel cells. *Sustainable Energy & Fuels*, 4(10):5238–5246, 2020.

[105] Andrew Cai and Zoe Rozario. Direct Ammonia Fuel Cells : A general overview, current technologies and future directions. *Johnson Matthey Technology Review*, 66(4):479–489, 10 2022.

[106] Ship and offshore No.6 (2021). Ammonia fuel cells for deep-sea shipping.

[107] M. Tayyeb Javed, Naseem Irfan, and B. M. Gibbs. Control of combustion-generated nitrogen oxides by selective non-catalytic reduction, 5 2007.

[108] Lingling Zhai, Chiu Shek Wong, Honglei Zhang, Pei Xiong, Xiangdang Xue, Yiu

Lun Ho, Cuidong Xu, Yat Chi Fong, Jie Mei, Wing Wa Chan, Shu Chuen Ip, Shuangxia Niu, Shu Ping Lau, Ka Wai Eric Cheng, and Molly Meng-Jung Li. From lab to practical: An ammonia-powered fuel cell electric golf cart system. *Chemical Engineering Journal*, 452:139390, 1 2023.

[109] EJ Cairns, EL Simons, and AD Tevebaugh. Ammonia–oxygen fuel cell. *Nature*, 217(5130):780–781, 1968.

[110] Georgina Jeerh, Peimiao Zou, Mengfei Zhang, and Shanwen Tao. Perovskite oxide LaCr0.25Fe0.25Co0.5O3-δ as an efficient non-noble cathode for direct ammonia fuel cells. *Applied Catalysis B: Environmental*, 319:121919, 12 2022.

[111] E Agel, J Bouet, and J.F Fauvarque. Characterization and use of anionic membranes for alkaline fuel cells. *Journal of Power Sources*, 101(2):267–274, 10 2001.

[112] J.F. Fauvarque, S. Guinot, N. Bouzir, E. Salmon, and J.F. Penneau. Alkaline poly(ethylene oxide) solid polymer electrolytes. Application to nickel secondary batteries. *Electrochimica Acta*, 40(13-14):2449–2453, 10 1995.

[113] Mônica H.M.T. Assumpção, Ricardo M. Piasentin, Peter Hammer, Rodrigo F.B. De Souza, Guilherme S. Buzzo, Mauro C. Santos, Estevam V. Spinacé, Almir O. Neto, and Júlio César M. Silva. Oxidation of ammonia using PtRh/C electrocatalysts: Fuel cell and electrochemical evaluation. *Applied Catalysis B: Environmental*, 174-175:136–144, 9 2015.

[114] Rong Lan and Shanwen Tao. Direct Ammonia Alkaline Anion-Exchange Membrane Fuel Cells. *Electrochemical and Solid-State Letters*, 13(8):B83, 2010.

[115] Ben Achrai, Yun Zhao, Teng Wang, Gal Tamir, Reza Abbasi, Brian P Setzler, Miles Page, Yushan Yan, and Shimshon Gottesfeld. A direct ammonia fuel cell with a koh-free anode feed generating 180 mw cm- 2 at 120° c. *Journal of The Electrochemical Society*, 167(13):134518, 2020.

[116] Teng Wang, Yun Zhao, Brian P. Setzler, Reza Abbasi, Shimshon Gottesfeld, and Yushan Yan. A high-performance 75 W direct ammonia fuel cell stack. *Cell Reports Physical Science*, 3(4):100829, 4 2022.

[117] Georgina Jeerh, Peimiao Zou, Mengfei Zhang, and Shanwen Tao. Optimization of a Perovskite Oxide-Based Cathode Catalyst Layer on Performance of Direct Ammonia Fuel Cells. *ACS Applied Materials & Interfaces*, 15(1):1029–1041, 1 2023.

[118] Yun Zhao, Teng Wang, Brian P. Setzler, Reza Abbasi, Junhua Wang, and Yushan Yan. A High-Performance Gas-Fed Direct Ammonia Hydroxide Exchange Membrane Fuel Cell. *ACS Energy Letters*, 6(5):1996–2002, 5 2021.

[119] Feng Jiao and Bingjun Xu. Electrochemical ammonia synthesis and ammonia fuel cells. *Advanced Materials*, 31(31):1805173, 2019.

[120] Yi Li, Hemanth Somarajan Pillai, Teng Wang, Sooyeon Hwang, Yun Zhao, Zhi Qiao, Qingmin Mu, Stavros Karakalos, Mengjie Chen, Juan Yang, Dong Su, Hongliang Xin, Yushan Yan, and Gang Wu. High-performance ammonia oxidation catalysts for anion-exchange membrane direct ammonia fuel cells. *Energy & Environmental Science*, 14(3):1449–1460, 2021.

[121] Sapir Willdorf-Cohen, Avital Zhegur-Khais, Julia Ponce-González, Saja Bsoul-Haj, John R Varcoe, Charles E Diesendruck, and Dario R Dekel. Alkaline stability of anion-exchange membranes. *ACS Applied Energy Materials*, 2023.

[122] Zijun Hu, Qiangfeng Xiao, Dongdong Xiao, Ziming Wang, Fukang Gui, Yike Lei, Jie Ni, Daijun Yang, Cunman Zhang, and Pingwen Ming. Synthesis of Anti-poisoning Spinel Mn–Co–C as Cathode Catalysts for Low-Temperature Anion Exchange Membrane Direct Ammonia Fuel Cells. *ACS Applied Materials & Interfaces*, 13(45):53945–53954, 11 2021.

[123] Tong Huang, Xiaoyu Qiu, Junfeng Zhang, Xintian Li, Yabiao Pei, Haifei Jiang, Runfei Yue, Yan Yin, Zhongyi Jiang, Xiaosong Zhang, and Michael D. Guiver. Hydrogen crossover through microporous anion exchange membranes for fuel cells. *Journal of Power Sources*, 527:231143, 4 2022.

[124] Feng Jiao and Bingjun Xu. Electrochemical Ammonia Synthesis and Ammonia Fuel Cells. *Advanced Materials*, 31(31):1805173, 8 2019.

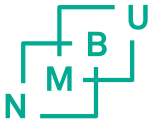

Norges miljø- og biovitenskapelige universitet
Noregs miljø- og biovitskapelege universitet
Norwegian University of Life Sciences

Postboks 5003
NO-1432 Ås
Norway